AMERICAN SOCIETY FOR MICROBIOLOGY | Journal of Bacteriology®

RESEARCH ARTICLE

MapA, a Second Large RTX Adhesin Conserved across the Pseudomonads, Contributes to Biofilm Formation by *Pseudomonas fluorescens*

Alan J. Collins,[a] Alexander B. Pastora,[a] T. Jarrod Smith,[a] George A. O'Toole[a]

[a]Department of Microbiology and Immunology, Geisel School of Medicine at Dartmouth, Hanover, New Hampshire, USA

Alexander B. Pastora and T. Jarrod Smith contributed equally to this work.

ABSTRACT Mechanisms by which cells attach to a surface and form a biofilm are diverse and differ greatly among organisms. The Gram-negative gammaproteobacterium *Pseudomonas fluorescens* attaches to a surface through the localization of the large type 1-secreted RTX adhesin LapA to the outer surface of the cell. LapA localization to the cell surface is controlled by the activities of a periplasmic protease, LapG, and an inner membrane-spanning cyclic di-GMP-responsive effector protein, LapD. A previous study identified a second, LapA-like protein encoded in the *P. fluorescens* Pf0-1 genome: Pfl01_1463. Here, we identified specific growth conditions under which Pfl01_1463, here called MapA (medium adhesion protein A) is a functional adhesin contributing to biofilm formation. This adhesin, like LapA, appears to be secreted through a Lap-related type 1 secretion machinery, and its localization is controlled by LapD and LapG. However, differing roles of LapA and MapA in biofilm formation are achieved, at least in part, through the differences in the sequences of the two adhesins and different distributions of the expression of the *lapA* and *mapA* genes within a biofilm. LapA-like proteins are broadly distributed throughout the *Proteobacteria*, and furthermore, LapA and MapA are well conserved among other *Pseudomonas* species. Together, our data indicate that the mechanisms by which a cell forms a biofilm and the components of a biofilm matrix can differ depending on growth conditions and the matrix protein(s) expressed.

IMPORTANCE Adhesins are critical for the formation and maturation of bacterial biofilms. We identify a second adhesin in *P. fluorescens*, called MapA, which appears to play a role in biofilm maturation and whose regulation is distinct from the previously reported LapA adhesin, which is critical for biofilm initiation. Analysis of bacterial adhesins shows that LapA-like and MapA-like adhesins are found broadly in pseudomonads and related organisms, indicating that the utilization of different suites of adhesins may be broadly important in the *Gammaproteobacteria*.

KEYWORDS *Pseudomonas fluorescens*, RTX, adhesin, biofilm, cyclic di-GMP

Biofilm formation is a critical mode of growth for many microorganisms, including bacteria (1), archaea (2), and fungi (3). The mechanisms by which individual cells can attach to abiotic surfaces, and to each other, to form a biofilm are highly varied. However, in all cases, formation of a biofilm involves the production of adhesive molecules by the cells. These molecules are most commonly polysaccharide or protein based, and these factors remain adhered to the substratum while also often remaining tethered to the cells that produced them (4–8).

In bacteria, many different mechanisms of surface attachment by cells have been described. The biofilm matrix is typically composed of a variety of molecules, including a combination of polysaccharides, proteins, and extracellular DNA, used to join cells

Citation Collins AJ, Pastora AB, Smith TJ, O'Toole GA. 2020. MapA, a second large RTX adhesin conserved across the pseudomonads, contributes to biofilm formation by *Pseudomonas fluorescens*. J Bacteriol 202:e00277-20. https://doi.org/10.1128/JB.00277-20.

Editor Yves V. Brun, Université de Montréal

Address correspondence to George A. O'Toole, georgeo@dartmouth.edu.

Received 7 May 2020
Accepted 29 June 2020
Accepted manuscript posted online 6 July 2020
Published 25 August 2020

together into a biofilm (4, 9–12). In general, a combination of multiple molecules makes up the biofilm matrix, but some organisms use different molecules as their major biofilm matrix components. Examples include the production of a polysaccharide called *Vibrio* polysaccharide (VPS) and the matrix proteins RbmA, RbmC, and Bap1 by *Vibrio cholerae* (13–15) and the production of amyloid proteins called curli fibers by *Escherichia coli* (16). For many bacteria, biofilm formation is important for the effective colonization of their natural niches in the soil, on plants, or in the water column (17–19). Biofilm formation has also been implicated as an important virulence factor for many pathogenic bacteria (20–22). It is therefore important to understand both the mechanisms by which bacteria can form a biofilm and the ways in which that process is regulated.

An organism with one of the best-understood mechanisms of surface attachment and regulation of biofilm formation is *Pseudomonas fluorescens*. In *P. fluorescens*, surface attachment is achieved predominantly through the activity of a single large adhesion protein, LapA (23, 24). LapA is a noncanonical type 1-secreted, RTX adhesin which is composed of a C-terminal secretion signal as well as a central portion containing numerous repeat domains, multiple calcium binding domains, and a von Willibrand factor A domain that all contribute to adhesion (25–27). LapA also has an N-terminal globular domain that folds while the protein is in the process of being secreted, thus anchoring the protein in its TolC-like outer membrane pore (28, 29). LapA is an ~520-kDa adhesin (25–27) and was thus named the large adhesion protein A and for *lapa*, the Spanish word for limpet, a marine mollusk that attaches tightly to rocks and other surfaces (23). The localization of LapA to the cell surface is dependent on the activity of two regulatory proteins, namely, LapG, a periplasmic cysteine protease that can proteolytically process LapA, removing the globular N terminus and releasing LapA from the cell surface, and LapD, an inner membrane-localized GGDEF/EAL-containing, cyclic di-GMP (c-di-GMP)-responsive effector protein that binds LapG in response to cytoplasmic c-di-GMP, preventing LapG's access to the N terminus of LapA (25, 28, 30–34). Together, LapD and LapG function to transduce cytoplasmic c-di-GMP signals across the inner membrane and determine whether LapA is retained at the cell surface or not (28, 34, 35). While the biofilms formed by some lab strains and environmental isolates of *P. fluorescens* have been shown to contain appreciable levels of polysaccharides (36, 37), in the best studied lab strain, Pf0-1, *P. fluorescens* polysaccharides have not previously been shown to play an appreciable role in biofilm formation. Instead, LapA has been shown to be the key determinant of biofilm formation (23, 28, 31). The simplicity of the use of a single adhesin protein to determine surface attachment and biofilm formation has made *P. fluorescens* an attractive model system for the study of biofilm formation and its regulation by c-di-GMP.

In this study, we demonstrate that biofilm formation in *P. fluorescens* is not determined solely by the action of LapA but instead by the action of two, related proteins, LapA and the herein described medium adhesion protein A (MapA). We show that while these two proteins share much of the regulatory machinery controlling cell surface localization, the differences in transcriptional regulation, their differential expression within mature biofilms, and their distinct sizes and sequences suggest that these two large adhesins play different roles in the development of a mature biofilm by *P. fluorescens*. We also demonstrate that LapA- and MapA-like proteins can be found in various combinations in the *Gammaproteobacteria*.

RESULTS

LapA is not necessary for the formation of a biofilm under all medium conditions. Previous work characterizing the role of the adhesive protein LapA in biofilm formation had suggested that biofilm formation by *P. fluorescens* Pf0-1 is dependent on the function of LapA (23, 25, 28, 29). However, recent work by Smith et al. (29) indicated that *P. fluorescens* Pf0-1 encodes a second putative large adhesin. LapA is approximately 520 kDa, while this second adhesin, encoded by the Pfl01_1463 gene, is predicted to be approximately 300 kDa. We therefore named this new putative adhesin

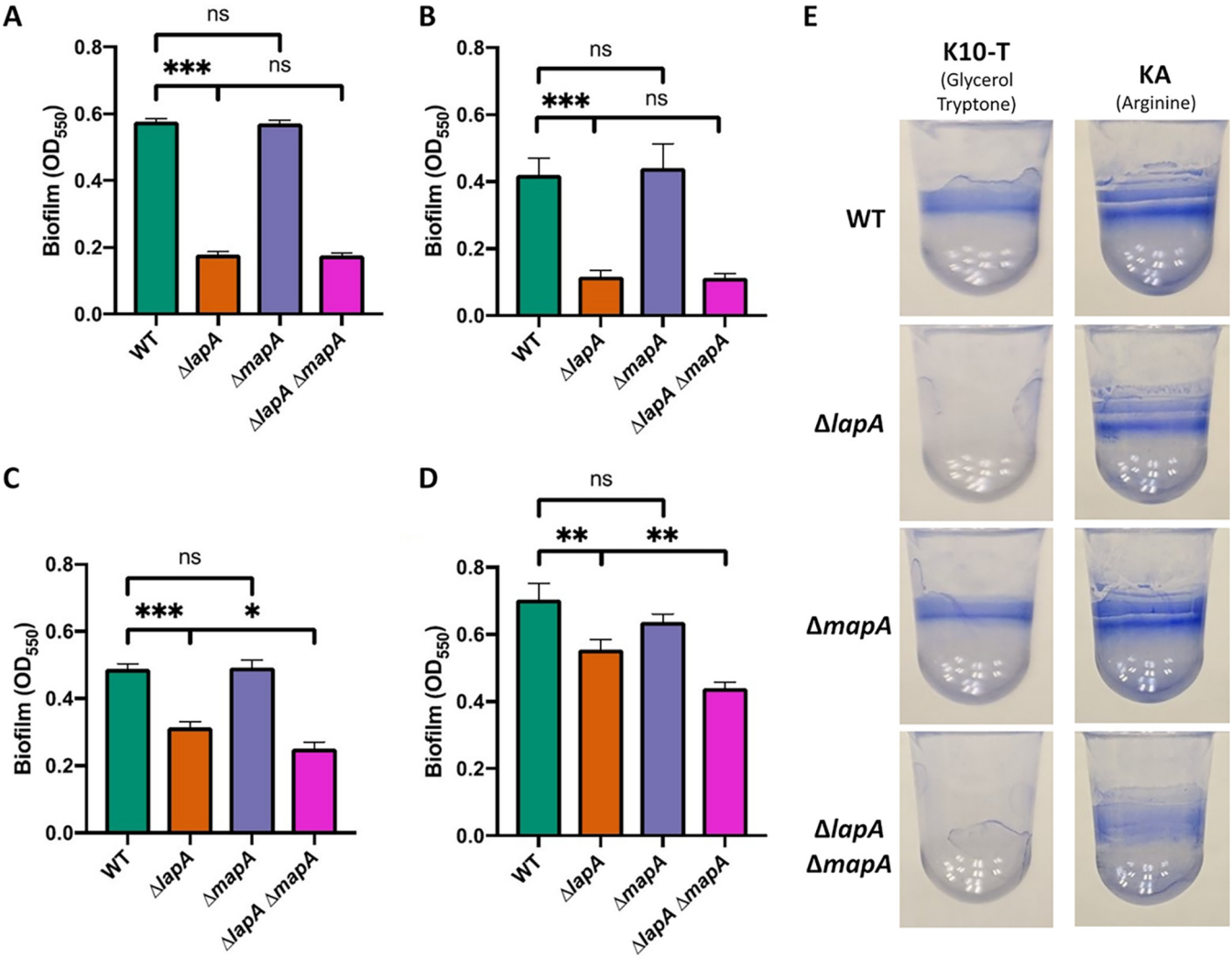

FIG 1 Biofilm formation by adhesin mutants. (A to D) Quantification of biofilm formed by WT *P. fluorescens* Pf0-1, Δ*lapA* and Δ*mapA* single mutants, and the Δ*lapA* Δ*mapA* double mutant after 6 h of growth in K10-T medium (A), 16 h of growth in K10-T medium (B), 6 h of growth in KA medium (C), and 16 h of growth in KA medium (D). For statistical tests, hypothesis testing was conducted in GraphPad Prism 8 using two-tailed *t* tests. *P* values are indicated by asterisks as follows: *, $P < 0.05$; **, $P < 0.01$; ***, $P < 0.001$; nonsignificant (ns), $P > 0.05$. (E) Representative image of biofilm formed by WT *P. fluorescens* Pf0-1 and Δ*lapA*, Δ*mapA*, and Δ*lapA* Δ*mapA* mutants after 16 h of growth in the indicated medium and stained with 0.1% (wt/vol) crystal violet.

MapA (medium adhesion protein A), since the data shown below support a role for MapA as a biofilm adhesin.

We first assessed biofilm formation by mutants lacking one or both of the *lapA* and *mapA* genes in K10-T medium, a high-phosphate medium containing glycerol and tryptone as carbon and nitrogen sources that is commonly used in studies of *P. fluorescens* Pf0-1 biofilm formation. After 6 h of growth in this medium, the Δ*mapA* mutant formed the same amount of biofilm as that of wild-type (WT) Pf0-1, while the Δ*lapA* mutant formed no biofilm, similarly to the Δ*lapA* Δ*mapA* double mutant (Fig. 1A). This pattern was also observed after 16 h of growth in K10-T medium (Fig. 1B and E).

In order to find a role for MapA in biofilm formation, we sought to assess the biofilm formed by a Δ*lapA* or Δ*mapA* single mutant or a Δ*lapA* Δ*mapA* double mutant under a growth condition that fosters robust biofilms. Arginine has been shown to strongly promote biofilm formation by *Pseudomonas* species, likely through stimulation of the production of c-di-GMP (38–41). In addition, arginine is commonly found in root exudates and is therefore likely encountered by *P. fluorescens* when growing in the soil (42–44). After trying several medium formulations (data not shown), we found that the condition under which a Δ*lapA* mutant is most capable of biofilm formation is a

modification of K10-T medium in which no glycerol or tryptone is added but rather it is supplemented with 0.4% (wt/vol) L-arginine HCl (here referred to as KA medium), as described in Materials and Methods. Of note, we have shown previously that growth on arginine increases the level of cellular c-di-GMP and stimulates biofilm formation by *Pseudomonas* (39, 41), perhaps accounting for our ability to observe an impact of MapA on biofilm formation in this medium formulation.

When grown in KA medium, WT *P. fluorescens* Pf0-1 can form a biofilm by 6 h, although less well than it can in K10-T medium (Fig. 1C). After 6 h of growth, the Δ*lapA* mutant has a significantly higher level of biomass attached to the well than the Δ*lapA* Δ*mapA* mutant, although the Δ*mapA* single mutant shows no reduction in biofilm compared to the WT. When cells were allowed to grow for 16 h in KA medium, the relative deficit in biofilm formation by the Δ*lapA* mutant was reduced, while the significant deficit of the Δ*lapA* Δ*mapA* mutant was still observed (Fig. 1D and E). In addition, the biofilm formed by the Δ*mapA* mutant in KA medium after 16 h of growth was slightly (but not significantly) lower than that of the WT ($P = 0.09$, unpaired two-tailed *t* test). Interestingly, when the Δ*lapA* Δ*mapA* mutant was grown in KA medium for 16 h, there was still modest diffuse staining observed in the well (Fig. 1E), perhaps indicating an additional factor contributing to biofilm formation under these conditions. These data indicate that MapA is capable of significantly contributing to biofilm under some medium conditions and is able to do so in the absence of LapA when grown in KA medium.

Genetic studies indicate that MapA localization is controlled by the regulatory proteins LapD and LapG. Localization of LapA to the cell surface is dependent on the activity of the proteins LapD and LapG. The structure of the N-terminal portion of LapA is essential for its retention in the outer membrane pore LapE and thus for anchoring LapA to the bacterial cell surface (25, 29). *In silico* analysis of the N-terminal portion of LapA and MapA indicates a high degree of sequence and secondary structure similarity as well as the presence of the functionally important TAAG motif required for LapG processing (35) (Fig. 2A, red box).

Previous work demonstrated that the regulatory protease, LapG, is capable of proteolytically processing the N-terminal portion of MapA *in vitro* (29). To assess the regulatory role of LapD and LapG in the localization of MapA, we examined the level of biofilm formation of mutants lacking *lapD* or *lapG* when grown in KA medium (Fig. 2B). We found that while a Δ*lapA* mutant can form a biofilm in KA medium, the biofilm is significantly reduced in a Δ*lapD* mutant compared to the Δ*lapA* mutant, consistent with LapD being required to prevent constitutive processing of LapA and MapA by LapG. We also observed a reduction in the biofilm formed by the Δ*lapAG* Δ*mapA* mutant compared to the Δ*lapAG* mutant, indicating that MapA does contribute to the biofilm formed under these conditions. Interestingly, when cells were grown in KA medium (Fig. 2B), no significant difference in biofilm formation was observed between the WT and the Δ*lapG* mutant or between the Δ*lapA* mutant and the Δ*lapAG* mutant. These data suggest that while LapG is capable of processing both LapA and MapA, cells grown in KA medium have very little LapG activity, so the loss of LapG does not lead to an appreciable increase in biofilm formation, in contrast to cells grown in K10-T medium (Fig. 2C). Finally, when grown in KA medium, the Δ*lapD* mutant forms less biofilm than the Δ*lapA* Δ*mapA* mutant, although this difference is not statistically significant when the *P* value is adjusted to control the family-wise error rate. This observation may indicate the existence of an additional, unknown, LapD-regulated factor that modestly contributes to biofilm formation under these conditions, an observation consistent with the biofilm data shown in Fig. 1D and E. Taken together, these genetic data are consistent with the previous biochemical data (29), indicating that MapA is a substrate of LapG and its localization is likely regulated by LapD.

MapA is localized to the cell surface. The sequence similarity between the N termini of LapA and MapA, the role for MapA in biofilm formation, the impact of loss of function in LapD on MapA-dependent biofilm formation, as shown here, and the

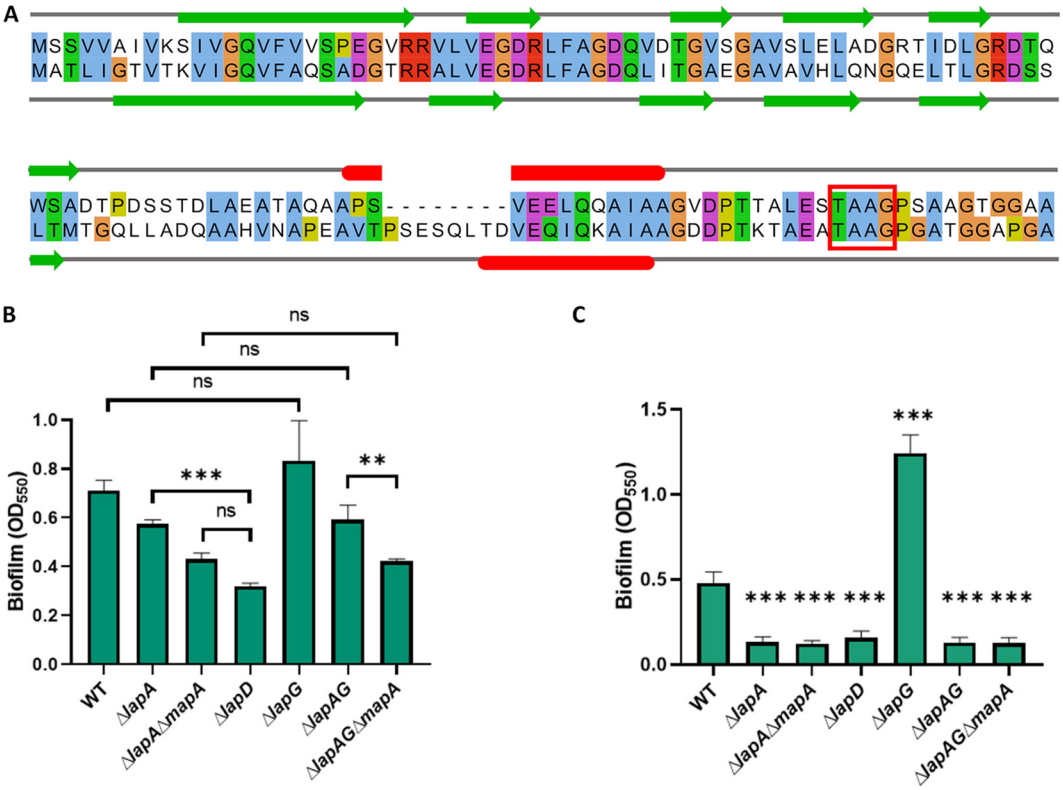

FIG 2 LapD and LapG contribute to MapA-dependent biofilm formation. (A) Alignment of LapA and MapA N-terminal portions generated using MUSCLE (65) and visualized using Jalview (85) with secondary structure prediction using JPred4 (83). Similar residues are indicated by color. Predicted secondary structure is indicated by colored shapes: green arrows, beta sheets; red bars, alpha helix. The LapG processing site TAAG is indicated by a red box. (B) Quantification of biofilm assay assessing biofilm formation of adhesin and regulatory mutants grown for 16 h in KA medium. (C) Quantification of biofilm assay assessing biofilm formation of adhesin and regulatory mutants grown for 16 h in K10-T medium. For statistical tests, hypothesis testing was conducted in GraphPad Prism 8 using two-tailed *t* tests with Holm-Sidak's multiple comparison correction. *P* values are indicated by asterisks as follows: **, $P < 0.01$; ***, $P < 0.001$; ns, $P > 0.05$. In panel C, all asterisks denote *P* values of *t* tests between WT and the indicated mutant with Holm-Sidak's multiple comparison correction.

published observation that the N terminus of MapA is processed by LapG (29) are all consistent with the conclusion that MapA is a cell surface-localized adhesin. To assess the cell surface localization of MapA, we built a hemagglutinin (HA)-tagged variant of MapA at the native locus on the chromosome, and this strain showed no difference in biofilm formation compared to the untagged WT strain when grown in KA medium (Fig. 3A, left); we similarly saw no impact of the HA tagging of MapA on the biofilm formed in the *lapA* mutant background (Fig. 3A, right).

We next performed dot blot studies that specifically assess the MapA associated with the bacterial cell surface. In these studies, cells are harvested by centrifugation, washed, spotted on a nitrocellulose filter, and then probed with an antibody to the HA-tagged variant to MapA. As shown in Fig. 3B and C, while no signal is detected for the untagged WT strain (left), a strong signal is detected for the strain carrying the HA-tagged MapA (center), and as an additional negative control, this signal is absent from a strain in which both the *lapA* and *mapA* genes are deleted (right). These data are consistent with MapA, like LapA, being cell surface localized.

Genetic evidence that components of the T1SS of LapA may be promiscuous. Homologs of LapA are commonly encoded adjacent to their cognate type 1 secretion system (T1SS) (23, 45). This is also true for MapA. The *mapA* gene is adjacent to three genes encoding a putative T1SS (Fig. 4). We have named these genes *mapB*, *mapC*, and *mapE*, encoding a predicted inner membrane-spanning ABC transporter, a membrane fusion protein, and an outer membrane pore protein, respectively. Given that TolC, a homolog of LapE and MapE, is capable of functioning in association with multiple

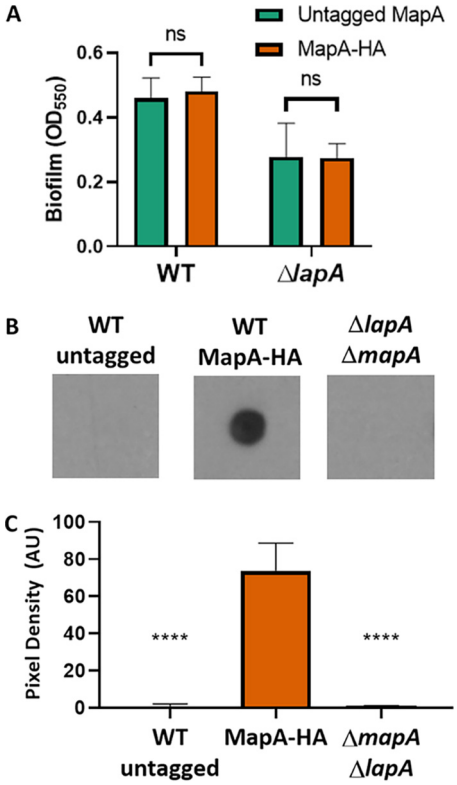

FIG 3 MapA is localized to the cell surface. (A) Quantification of crystal violet staining of wells of a 96-well plate after 16 h of growth in KA. Results for *P. fluorescens* Pf0-1 in both the untagged MapA and the tagged MapA variant bearing 3 tandem HA tags are shown. The phenotype is shown either in strains carrying a functional LapA or in a strain for which the *lapA* gene has been deleted. When compared using Student's *t* test, neither *P. fluorescens* Pf0-1 ($P = 0.25$) nor the Δ*lapA* mutant ($P = 0.9$) formed a significantly different level of biofilm when bearing an HA-tagged variant of MapA. (B) Representative dot blot of cell surface-localized MapA for the indicated strains. The WT (untagged strains) and a strain deleted for both the *mapA* and *lapA* genes serve as negative controls. (C) Three independent dot blot experiments were quantified using ImageJ as follows. The pixel values for the blots were inverted for ease of plotting. The region of interest (ROI) was defined for the control LapA dot blot (not shown), and then the mean gray value was determined for each spot using the predefined ROI. The background was subtracted from each spot; the background was determined by measuring the mean gray value in a section of the blot not containing any samples. The adjusted mean pixel density was plotted here for three biological replicates. There was a significant reduction in signal for both control strains compared to the strain expressing MapA-HA as assessed by *t* test. ****, $P < 0.001$; ns, $P > 0.05$.

different ABC transporters and membrane fusion proteins (46–50) and the sequence similarity between these proteins (both LapE and MapE share roughly 35% similarity with TolC), we next sought to assess the extent to which LapA and MapA might share the components of their secretion systems. To investigate the ability of LapA and MapA to be secreted through either secretion machinery, we assessed the level of biofilm formed by mutants lacking combinations of adhesin and secretion machinery genes grown for 16 h in KA.

The biofilms produced by the Δ*lapA*, Δ*mapA*, and Δ*mapE* mutants were not different from one another but were significantly reduced compared to that produced by the WT (Fig. 5A). The biofilm formed by the Δ*lapA* Δ*mapE* mutant was reduced compared to those produced by both the Δ*lapA* and Δ*mapE* mutants but was not as low as that produced by the Δ*lapA* Δ*mapA* or Δ*lapE* Δ*mapE* mutants. This intermediate degree of biofilm formation indicates that when LapA and MapE are absent, MapA is likely able to be secreted, at least in part, via some portion of the LapBCE T1SS and thereby contribute to biofilm formation.

Next, we assessed the ability of LapA to be secreted in the absence of LapE (Fig. 5B). The Δ*lapE* Δ*mapA* mutant formed a biofilm that was not different from that formed by

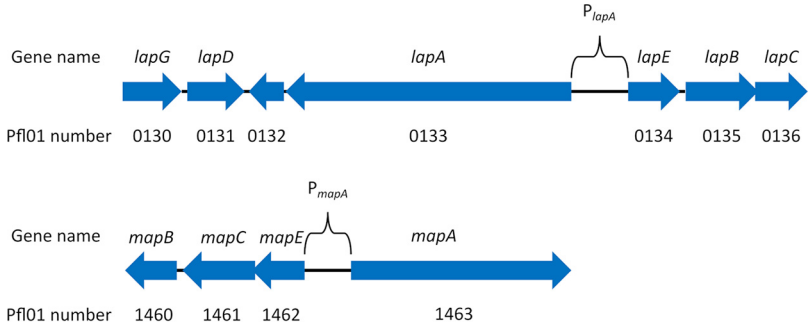

FIG 4 Schematic of the *lap* and *map* loci. The organization of the genes encoding the LapA and MapA adhesins and their secretion machinery is shown. Gene names are indicated above the arrows, and the *P. fluorescens* Pfl0-1 gene numbers are indicated below the arrows. Arrows indicate the location and direction of transcription of the ORFs. Arrow direction indicates the orientation of the gene in the genome.

the Δ*lapE* Δ*mapE* mutant. This observation suggests that while MapA may utilize some portion of the LapBCE T1SS, LapA is likely not secreted through the MapBCE T1SS. Additionally, it was observed that deletion of the *lapE* gene resulted in a greater decrease in the biofilm formed than the deletion of the *lapA* gene. This supports a model in which MapA is capable of being secreted through both secretion systems and is therefore able to partially suppress the impact of the loss of LapA on biofilm formation. Alternatively, the differential expression of LapA and MapA may also explain the inability of LapA to use the Map secretion machinery.

LapA and MapA are both required for the typical three-dimensional structure of the biofilm. We next sought to elucidate the functional significance of encoding two large adhesins in the context of the formation of a mature biofilm using a flow cell system. After 96 h of growth in a modified version of the previously described BMM medium (51) (see Materials and Methods) in the microfluidic chamber, the WT forms a thick biofilm that fills most of the flow cell chamber (Fig. 6A). The Δ*lapA* mutant is severely deficient in biofilm formation, and only small clumps of cells are observed

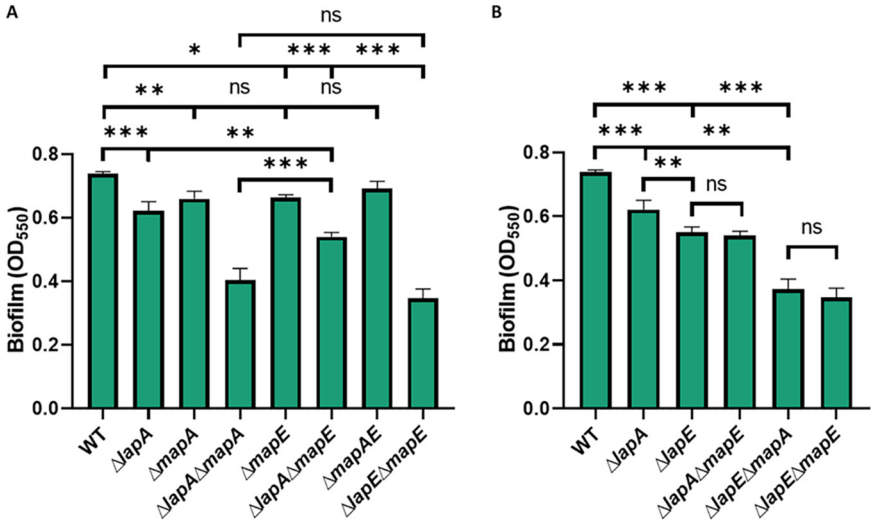

FIG 5 Genetic evidence that MapA can utilize the Lap secretion system. (A) Biofilm formation by strains in KA medium carrying mutations in adhesin genes and genes encoding the Map secretion system outer membrane pore component. (B) Biofilm formation in KA medium for strains carrying mutations in adhesin genes and genes encoding the Lap secretion system outer membrane pore component. For statistical tests, hypothesis testing was conducted in GraphPad Prism 8 using two-tailed *t* tests with Holm-Sidak's multiple comparison correction. *P* values are indicated by asterisks as follows: *, $P < 0.05$; **, $P < 0.01$; ***, $P < 0.001$; ns, $P > 0.05$.

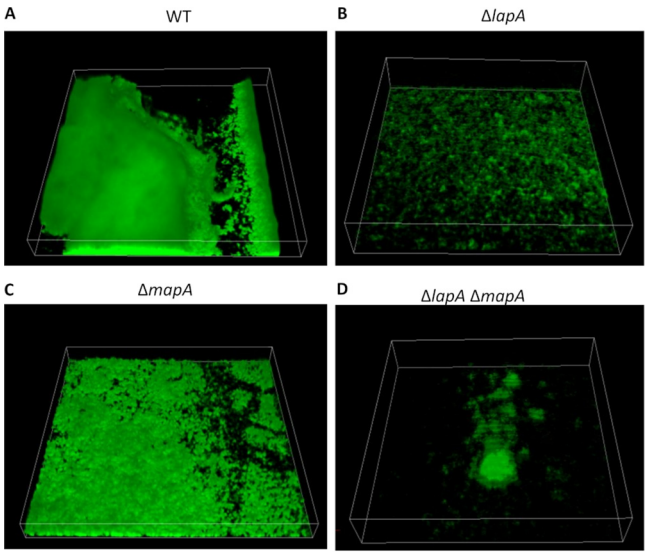

FIG 6 Confocal spinning-disk microscopy images of biofilm formed by adhesin mutants in flow cells. The indicated strains were grown as described in Materials and Methods and incubated at room temperature under constant flow for 96 h before imaging. Shown are representative images taken from one of two biological replicates. (A) The WT forms a thick biofilm that fills most of the flow cell chamber. (B) The Δ*lapA* mutant is severely deficient in biofilm formation, and only small clumps of cells are observed attached to the surface. (C) The Δ*mapA* mutant appears able to attach to the surface of the chamber, but the thickness of the biofilm is reduced compared to that of WT. (D) The Δ*lapA* Δ*mapA* mutant results in a biofilm comprised of sparsely distributed clumps of cells.

attached to the surface (Fig. 6B), as reported previously (23). The Δ*mapA* mutant appears able to attach to the surface of the chamber, but the thickness of the biofilm is reduced compared to that of the WT (Fig. 6C). Finally, the Δ*lapA* Δ*mapA* mutant results in a biofilm comprised of sparsely distributed clumps of cells (Fig. 6D). Together, these clear deficiencies in biofilm structure support a role for both adhesins in the formation of the biofilm.

The *lapA* and *mapA* genes are differentially expressed in a *P. fluorescens* Pf0-1 biofilm. Given the differential impact on biofilm formation for the *lapA* and *mapA* mutants, we hypothesized that LapA and MapA may be produced in different regions of a biofilm. In order to test this hypothesis, we constructed a reporter strain in which the promoter of each adhesin is driving the expression of a different fluorescent protein at a neutral site on the chromosome, while the native loci remain unchanged and thus functional. In this strain, the promoter of the *lapA* gene drives expression of green fluorescent protein (GFP) while the promoter of the *mapA* gene drives production of mRuby. Thus, this strain produces LapA and MapA from their native loci, while the GFP and mRuby constructs function as reporters of the activity of the *lapA* and *mapA* promoters, respectively. Figure 7A depicts a graphical representation of this adhesin reporter construct.

We grew this adhesin reporter strain in microfluidic devices under constant flow in a variant of the KA medium (see Materials and Methods for details) for 96 h and then imaged the biofilms formed by spinning-disk confocal microscopy to assess expression of the *lapA* or *mapA* reporters (Fig. 7B). Figure 7B shows a typical field of view in which a thick region of biofilm can be seen spanning from the bottom to the top of the center of the field of view, while the regions on either side of this central area of dense biofilm are visibly more porous and thinner. We found that only *lapA* is expressed in the areas where the biofilm is thin or less dense (Fig. 7B, green, right portion of the field of view), whereas robust *lapA* and *mapA* expression could both be detected in regions where the biofilm is thicker and denser (Fig. 7B, magenta). The expression of the *mapA* gene is localized to this dense biofilm region and is not observed in the more porous regions of the biofilm. In addition, *mapA* expression seemed to be localized to the region

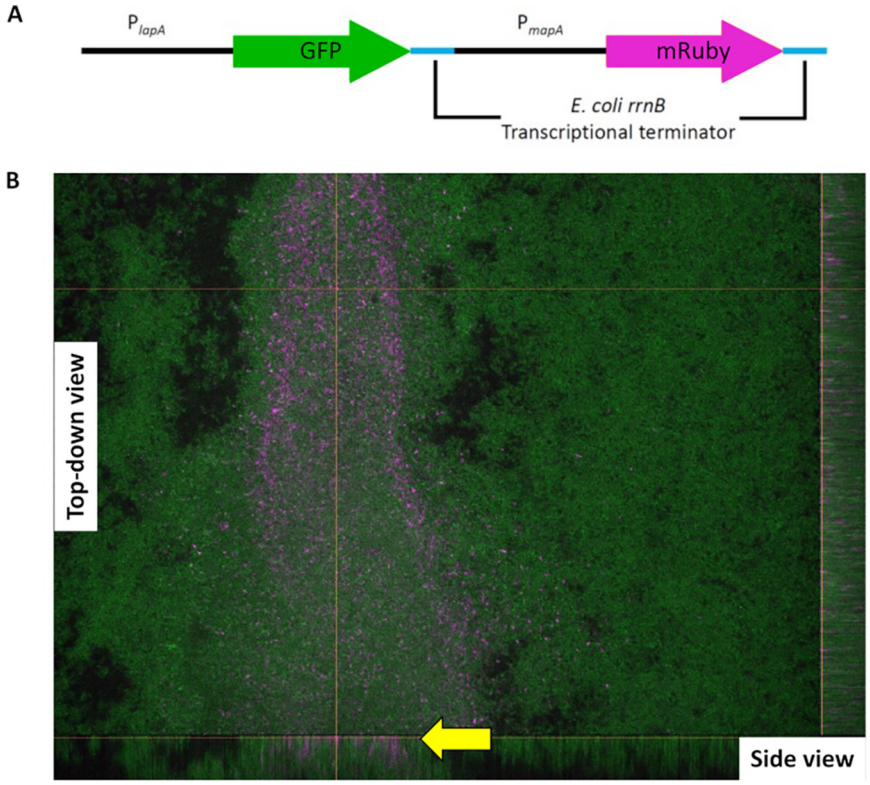

FIG 7 Differential expression of *lapA* and *mapA* genes in a biofilm. (A) Schematic of adhesin reporter construction indicating the promoter and the gene encoding the fluorescent protein gene. P_{lapA} is driving the expression of the green fluorescent protein gene, and P_{mapA} is driving the expression of the mRuby gene. Both fluorescent protein genes have a transcriptional terminator of the *rrnB* gene from *E. coli* downstream of the genes to prevent transcriptional readthrough. (B) Confocal image of a biofilm grown in a microfluidic device. The image of a 96-h biofilm was taken with a 40× oil immersion lens objective. Green is the GFP channel excited by a 488-nm laser and indicates *lapA*-expressing cells. Magenta is the mRuby channel excited by a 560-nm laser and indicates *mapA*-expressing cells. Shown is a representative image taken from one of two biological replicates.

closest to the point of attachment to the glass cover slip, as shown by the side projections on the right and the bottom of Fig. 7B (arrow).

The observations that LapA and MapA seem to be capable of supporting biofilm formation under different growth conditions and are both required for proper three-dimensional biofilm structure support a model wherein these two adhesins play different roles during biofilm formation. However, it is not clear from these data whether those different roles are due solely to differences in transcriptional regulation and that LapA and MapA are otherwise functionally redundant or, alternatively, that the proteins have distinct functions/roles in the context of biofilm formation due to their distinct amino acid sequences. To distinguish between these possibilities, we created a strain in which *mapA* expression is placed under the control of the *lapA* promoter, referred to as Pswap. The region described here as the *lapA* promoter is defined as spanning from the base adjacent to the *lapE* open reading frame (ORF) to the base adjacent to the *lapA* ORF (Fig. 4). The region described as the *mapA* promoter region is the equivalent region spanning from the base adjacent to the *mapE* ORF to the base adjacent to the *mapA* ORF (Fig. 4). We reasoned that this construct would lead to both *mapA* and the *mapBCE* genes encoding its cognate T1SS being transcriptionally regulated in a fashion similar to that of *lapA* and its cognate T1SS. We hypothesized that LapA and MapA function differently due to their different amino acid sequences and that, therefore, placing *mapA* under the transcriptional control of the *lapA* promoter would not rescue the biofilm defect of the Δ*lapA* mutant.

We tested biofilm formation of the WT and the Δ*lapA*, Pswap, and Δ*lapA* Pswap mutants when grown in KA medium for 6 and 16 h (Fig. 8A and B). If MapA were

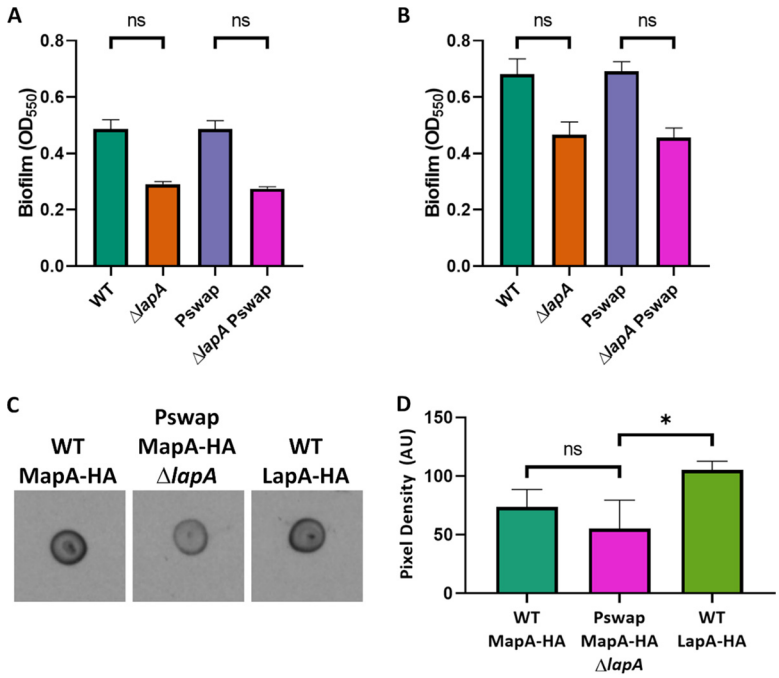

FIG 8 Expressing *mapA* under the control of the *lapA* promoter does not rescue loss of LapA function. (A and B) Quantification of biofilm formed by WT *P. fluorescens* Pf0-1 and Δ*lapA*, Pswap, and Δ*lapA* Pswap mutants after 6 h of growth in KA medium (A) or 16 h of growth in KA medium (B). (C) Cell surface expression of MapA in the WT and Pswap strains. The cell surface expression of LapA is shown as an additional control. Shown is one representative experiment of three biological replicates. (D) Quantification of the cell surface expression of HA-MapA in the WT and Pswap strains and of HA-LapA in the WT strain, as indicated. Quantification was performed as described in the legend for Fig. 3. For statistical tests, all hypothesis testing was conducted using a two-tailed *t* test. *, $P < 0.05$; ns, $P > 0.05$.

functionally equivalent to LapA, then we would expect the Δ*lapA* Pswap mutant to behave like a complemented *lapA* mutant and form approximately WT levels of biofilm. Instead, we observed no increase in biofilm formation between the Δ*lapA* and Δ*lapA* Pswap mutants at either time point (Fig. 8A and B).

To confirm that MapA was expressed and, more importantly, surface localized in the Δ*lapA* Pswap strain, we performed a dot blot experiment as described above. We found that the Δ*lapA* Pswap strain did indeed yield cell surface HA-MapA at a level that was not significantly different from the level of MapA produced by the WT strain (Fig. 8C and D, compare left and center of panel C). As an additional positive control, we also blotted for the cell surface levels of LapA in a strain carrying the HA-LapA-expressing construct (Fig. 8C, right). Given that we observed no change in biofilm formation between the *lapA* and Δ*lapA* Pswap mutants (Fig. 8A and B) and that the level of MapA in the Pswap strain was ~75% that of the WT strain but not significantly different, the simplest explanation for these observations is that MapA cannot functionally substitute for LapA.

Lap-like systems are broadly distributed throughout the *Proteobacteria*. The use of multiple adhesins in biofilm formation has been described in other organisms, for example, BapA and SiiE in *Salmonella enterica* (52–54) and LapA and LapF in *Pseudomonas putida* (45, 55–57). We were therefore interested in assessing how widespread this phenomenon may be throughout the bacterial domain in the context of LapA-like adhesins. To assess the distribution of these proteins, we modified a previously described approach to identify LapD and LapG homologs in other organisms and then examined those genomes for evidence of RTX adhesins that may be targets of the LapG homolog in the same organism (29). (See Materials and Methods for a description of this approach. All code and the raw data used in this analysis are available at https://github.com/GeiselBiofilm/Collins-MapA.)

TABLE 1 Number of genomes found to encode both putative LapD and LapG homologs in each of the given taxa

Taxon	No. of genomes encoding predicted LapD and LapG homologs/total no. of genomes (%)
Gammaproteobacteria	2,779/23,115 (12)
Betaproteobacteria	435/16,142 (2.7)
Alphaproteobacteria	301/12,355 (2.4)
Deltaproteobacteria/Epsilonproteobacteria	173/11,567 (1.5)
Zetaproteobacteria	23/43 (53)
Hydrogenophilalia	10/24 (42)
Deferribacteres	4/7,688 (0.05)
Bacteroidetes/Chlorobi group	1/499 (0.2)
Nitrospira	1/406 (0.2)

Using this approach, we identified 3,740 unique species encoding both LapD and LapG homologs. We next retrieved all available complete, annotated protein coding sequences for organisms of LapD- and LapG-encoding organisms that are available in the NCBI GenBank database. The phylogenetic class classification of these organisms is indicated in Table 1. The vast majority of these organisms whose genome encodes a LapA-like protein are members of the *Proteobacteria*, with most of those being members of the *Gammaproteobacteria*. The observation that we identified more organisms that encode putative LapD and LapG homologs in the *Gammaproteobacteria* than in other *Proteobacteria* is not necessarily indicative of an enrichment of these proteins in that class, as only 12% of *Gammaproteobacteria* represented in the GenBank database were found to encode LapD and LapG homologs. Indeed, 53% of the *Zetaproteobacteria* and 42% of the *Hydrogenophilalia* were found to encode both LapD and LapG, indicating that this system may be more highly represented in classes other than the *Gammaproteobacteria*. However, we identified almost no LapD and LapG homologs outside the *Proteobacteria* (Table 1), indicating that these proteins may be largely restricted to this phylum.

Having collected a list of LapD- and LapG-encoding organisms, we next retrieved amino acid sequences for all annotated genes in these organisms and searched these sequences for features that identify them as putative LapA-like proteins (see Materials and Methods for details). Briefly, the criteria for this characterization are the following: (i) having a size in excess of 1,000 amino acids, (ii) the presence of putative RTX repeats in the C-terminal portion of the protein, and (iii) the presence of a putative LapG cleavage site in the N-terminal portion of the protein. Through this search, we identified 1,020 organisms encoding predicted LapA-like proteins in addition to LapG and LapD homologs (see File S1 in the supplemental material). Through this approach, we were able to identify LapA-like proteins that have been previously described (55, 58–60), supporting the utility of this approach. Among organisms found to encode LapA-like proteins, approximately one-quarter were found to encode multiple LapA-like adhesins (Table 2). Interestingly, while many LapD- and LapG-encoding organisms encoded proteins that could be identified as LapA-like proteins, 2,720 organisms in our data set were found to encode LapD and LapG homologs but were not found to encode proteins that we could readily identify as LapA-like by use of our criteria, which could be due to the lack of such proteins or the difficulties in annotation of such large adhesins.

TABLE 2 Number of putative LapA-like adhesins predicted to be encoded in genomes in which putative LapD and LapG homologs were identified

No. of adhesins	No. of organisms
1	352
2	109
3	20
4	3

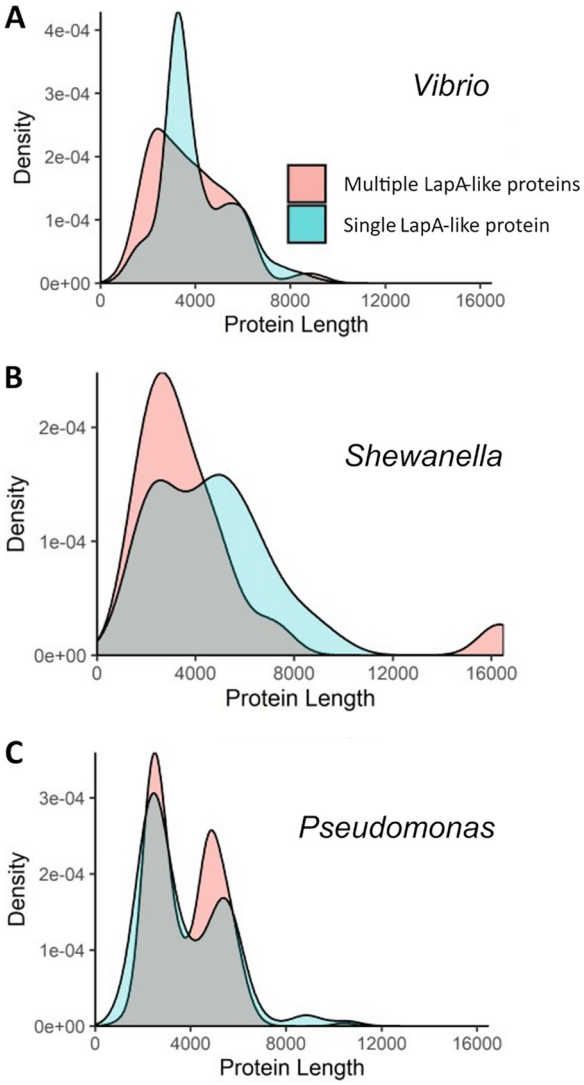

FIG 9 Size distribution of LapA-like proteins encoded by selected genera. All organisms found to encode both LapD and LapG and putative LapA-like proteins were grouped based on whether they are predicted to encode a single or multiple LapA-like proteins. We then assessed the distribution of the protein sizes of adhesins encoded by organisms with a single (blue shading) or multiple adhesins (orange shading). Shown are density plots representing the size distributions of LapA-like proteins found in the following genera: *Vibrio* (A), *Shewanella* (B), and *Pseudomonas* (C).

Pseudomonads encode LapA-like proteins with a distinct size distribution. RTX adhesins are typically large and are often the largest proteins produced by the bacteria in which they are found. Most of the length of these proteins is composed of tandem repeats. These repeats have in some cases been described to function as extender domains which hold the adhesive C-terminal domains far away from the cell surface (61, 62). Thus, while the functions of the various domains of LapA-like proteins are still in most cases unclear, the protein length may be an important characteristic. We therefore sought to assess the distribution of LapA-like protein sizes found within the three most highly represented genera in our data set, *Vibrio*, *Shewanella*, and *Pseudomonas* (Fig. 9). By plotting the distribution of LapA-like proteins, we can assess the sizes of adhesins encoded by organisms containing one or more such proteins.

LapA-like proteins encoded by *Vibrio* species with just one such protein exhibit a striking peak at a length of around 3,000 amino acids and a shoulder at around 5,000 amino acids (Fig. 9A). The major peak of organisms encoding a single LapA-like protein corresponds to a large number of *V. cholerae* isolates, including *V. cholerae* O1 biovar

El Tor, that encode an almost identical adhesin, while the shoulder at around 5,000 amino acids corresponds to a variety of different species. Interestingly, there is some diversity in the number and size of LapA-like proteins encoded by *V. cholerae* isolates, with some encoding two proteins and others just one such protein. In addition, there appear to be several distinct LapA-like variants encoded among isolates of *V. cholerae*. Some of these variant proteins appear to share very little sequence similarity to one another, while others appear to be mostly identical to another variant, differing mostly due to a large indel. For example, the LapA-like protein encoded by the *V. cholerae* O1 biovar El Tor is highly similar to a LapA-like protein encoded by *V. cholerae* TMA 21, but the El Tor protein is ~880 amino acids shorter. How these putative LapA-like proteins differ functionally from one another is unclear. However, the variation seen within the *V. cholerae* species may indicate that this protein is important for adaptation to different lifestyles of these organisms.

Within the genus *Shewanella*, no one species is represented dramatically more than any other in our data set. Accordingly, we do not see a dramatic peak in the protein size distribution corresponding to the adhesin encoded by a single species. Most of the species within this genus encode proteins that differ from those of other species both in size and at the sequence level, leading to a smooth curve when the size distribution is plotted (Fig. 9B). Interestingly, the largest LapA-like protein in our data set is encoded by *Shewanella woodyi* ATCC 51908 by the gene Swoo_0477. This protein is predicted to be 16,322 amino acids, which is over 5,000 amino acids longer than the next longest protein we identified as a LapA-like protein. While we are not aware of any experimental evidence to support the enormous size of this protein, it is nonetheless to our knowledge the largest predicted LapA-like protein.

The distribution of protein sizes observed within the *Pseudomonas* genus has a bimodal distribution, with peaks around 3,000 and 5,000 amino acids, the approximate sizes of MapA and LapA, respectively, among both organisms that encode a single and multiple LapA-like proteins (Fig. 9C). There are many isolates in our data set that have not been assigned a species designation and which encode proteins with sizes approximately equal to that of LapA and MapA. These isolates may represent oversampling of a small number of species that could exaggerate the observed distribution. However, there are also a considerable number of *Pseudomonas* isolates with species designations that exhibit this pattern.

***Pseudomonas* species encoding multiple LapA-like proteins are mostly *P. fluorescens* lineage members.** Having identified which *Pseudomonas* species encode LapD, LapG, and LapA-like proteins, we next sought to assess the phylogenetic distribution of these proteins within the genus. We therefore constructed a phylogenetic tree of the *Pseudomonas* species that are represented in the GenBank database (Fig. 10). The phylogenetic tree presented here has a topology similar to that of trees generated through the same approach in previous studies (63, 64) (see Fig. 10 legend and Materials and Methods for details).

Through our analysis, we identified LapD and LapG homologs throughout the *P. aeruginosa* and *P. fluorescens* lineages of the *Pseudomonas* genus (Fig. 10, innermost ring). However, LapD and LapG homologs were identified in only 2 of the 17 (11.7%) representatives of the *Pseudomonas pertucinogena* lineage, and only one of those was found to encode a LapA-like protein. Within the *P. aeruginosa* and *P. fluorescens* lineages, roughly the same proportions of species were found to encode LapD and LapG (56% and 59%, respectively). In addition, the proportions found to encode both LapD and LapG but no detectable LapA-like protein were also similar between the two lineages, with 9 of 50 species (18%) in the *P. aeruginosa* lineage and 26 of 147 species (17.7%) in the *P. fluorescens* lineage. Interestingly, these two lineages differ dramatically in number of adhesins detected in species that were found to encode LapD, LapG, and a LapA-like protein. Within the *P. aeruginosa* lineage, the number of species encoding a single adhesin is 15 (30%) and the number encoding more than one is 4 (8%). Within the *P. fluorescens* lineage, the number encoding a single adhesin is 32 (21%) and the

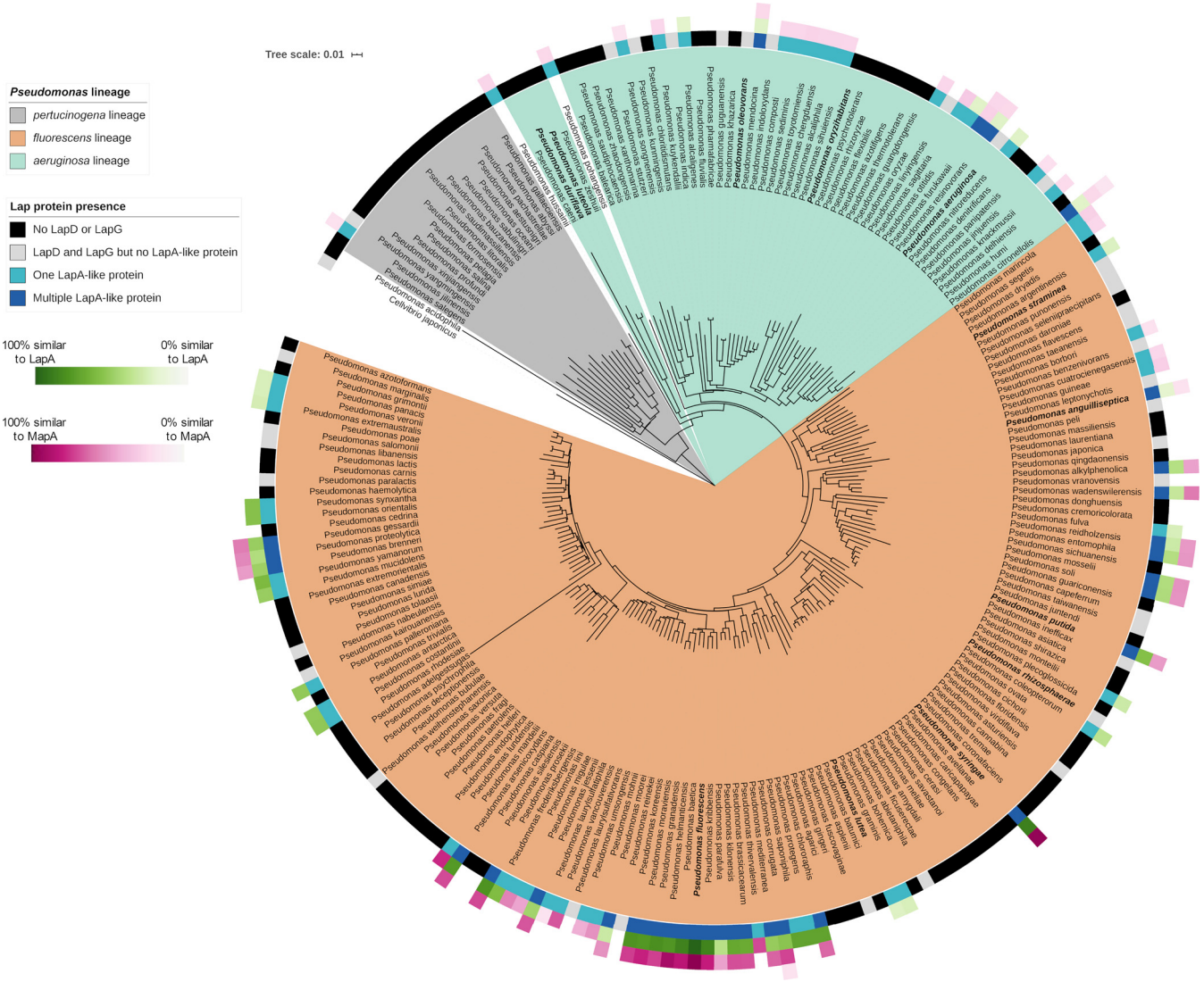

FIG 10 Phylogenetic distribution of the Lap proteins among members of the *Pseudomonas* genus. Shown is a phylogenetic tree of *Pseudomonas* lineages. The innermost colored ring around the tree indicates whether LapD and LapG are encoded by the indicated species (as determined by finding the intersection of the species lists retrieved from the NCBI Conserved Domain Database for pfam06035 and pfam16448 domains) and how many LapA-like proteins were identified in that species using the analysis described in Materials and Methods. The outermost three rings indicate the percent similarity between the LapA-like proteins identified in each species and either LapA or MapA. Amino acid sequences of putative LapA-like proteins were aligned with LapA and MapA in pairwise alignments using MUSCLE (65) (https://github.com/GeiselBiofilm/Collins-MapA/tree/master/Supplemental_File_Alignments), and the percent sequence similarity was determined by counting the positions identified as similar by the MUSCLE program. The percent similarity of whichever was most similar (either LapA or MapA) is indicated, with darker color indicating higher similarity. The order of the three rings indicating similarity with LapA and MapA is organized by the relative size of the LapA-like proteins encoded by each organism. The innermost of the three rings is the largest LapA-like protein encoded by that organism. The second and third rings represent alignments of the second- and third-largest LapA-like proteins, respectively, identified in organisms that are predicted to encode multiple LapA-like proteins. The multilocus sequence analysis (MLSA) phylogenetic tree here shows the clustering of representatives *Pseudomonas* species found in the GenBank database based on the analysis of concatenated alignments of 16S rRNA, *gyrB*, *rpoB*, and *rpoD* genes. Distance was calculated using the Jukes-Cantor model, and the tree was constructed using neighbor joining. The *P. aeruginosa*, *P. fluorescens*, and *P. pertucinogena* lineages described by Mulet et al. (64) are highlighted with the indicated colors. The namesake species of the groups described by García-Valdés and Lalucat (86) are in bold font. The *P. aeruginosa* and *P. fluorescens* lineages described by Mulet et al. (64) and the *P. pertucinogena* lineage described by Peix et al. (63) are also apparent in our tree and are indicated using the indicated shading (colored according to the lineages described by Peix et al. [63]). The most notable difference between the tree presented here and previously reported trees is the presence of a distinct *P. luteola* and *P. duriflava* clade, while Peix et al. (63) presented them as part of the monophyletic *P. aeruginosa* lineage. However, the placement of *P. luteola* within the *P. aeruginosa* lineage is not strongly supported. The study by Mulet et al. (64) placed *P. luteola* outside the *P. aeruginosa* lineage, and the bootstrap support for Peix et al. (63) positioning the *P. luteola* and *P. duriflava* clade within the *P. aeruginosa* lineage is less than 50%. Three other species were not present in previously published phylogenies of *Pseudomonas* and do not fit neatly into the three lineages described previously: *P. pohangensis*, *P. hussainii*, and *P. acidophila*. Both *P. pohangensis* and *P. hussainii* are positioned between the *P. pertucinogena* lineage and the other two lineages. *P. acidophila* is positioned outside the rest of the genus, consistent with a recent study that argued that *P. acidophila* should be reclassified as *Paraburkholderia acidophila* (87). While the *P. pertucinogena* lineage described by Peix et al. (63) is well supported by the tree we present here, the species *P. pertucinogena* is absent from our tree. This is because we included only species present in the GenBank database in our tree. At the time of writing, there is an available genome sequence record of *P. pertucinogena* (BioProject accession no. PRJNA235123), but the absence of an assembled genome from GenBank means that the organism was not included in our analysis of the distribution of LapA-like proteins. Nevertheless, the tree topology is similar overall to the previously reported trees outlined above.

number encoding multiple adhesins is 29 (20%). It is therefore clear that species encoding multiple LapA-like proteins are mostly found within the *P. fluorescens* lineage.

While species encoding LapD, LapG, and LapA-like proteins are found across both the *P. aeruginosa* and the *P. fluorescens* lineages, the distribution of these proteins within those lineages is not uniform. There are multiple clades within each lineage that seem to lack identifiable homologs for any of the three proteins. For example, within the *P. aeruginosa* lineage, the clade containing *P. luteola* and *P. duriflava* and the clade containing *P. oryzihabitans* are predominated by species that do not encode identifiable Lap proteins. Within the *P. fluorescens* lineage, the clade containing *P. syringae* is also predominated by species lacking identifiable Lap proteins. Interestingly, while species in the clade containing *P. syringae* mostly lack Lap proteins, *P. syringae* encodes both LapD and LapG as well as two identifiable LapA-like proteins.

LapA and MapA share high levels of sequence similarity with LapA-like proteins encoded by other *P. fluorescens* lineage members. Many members of the *P. fluorescens* lineage encode multiple LapA-like proteins, and the distribution of sizes of these proteins is similar to the sizes of LapA and MapA. Therefore, we hypothesized that the LapA-like proteins encoded by *Pseudomonas* species in our data set are similar to LapA and MapA, while those encoded by organisms from other genera are less similar to LapA and MapA. To assess this idea, we conducted pairwise alignments of the amino acid sequences of every LapA-like protein that we identified in our analysis with both LapA and MapA using MUSCLE v3.8 (65) (see File S2 in the supplemental material and https://github.com/GeiselBiofilm/Collins-MapA/tree/master/Supplemental_File_Alignments).

We found that within the *Pseudomonas* genus, many organisms encode adhesins that are highly similar to LapA and MapA (Fig. 10, rings of green and magenta squares). For example, *P. syringae* encodes two LapA-like proteins: the larger of the two is 87% identical and 90% similar to LapA, while the smaller of the two is 97% identical and 99% similar to MapA (Fig. 10; File S2). Interestingly, most of the organisms within the *P. fluorescens* lineage that encode multiple adhesins were found to encode proteins with very high similarity to LapA and MapA. However, LapA-like proteins encoded by members of the *P. aeruginosa* lineage have relatively lower similarity to LapA and MapA proteins.

Outside the *Pseudomonas* genus, the occurrence of proteins with very high similarity to LapA or MapA is lower. However, many organisms do encode proteins with moderate similarity (over 50% across the entire length of the protein) to LapA or MapA. In some cases, the similarity between these proteins is mostly localized to the N- and C-terminal portions of the proteins that contain the anchor domain and RTX repeats, respectively, which are characteristic of LapA-like proteins (66, 67). In other cases, it appears that similarity between adhesins is localized to the central portion of the protein. For example, the LapA-like protein encoded by *Aeromonas salmonicida* has 38% amino acid identity (68% similarity) to MapA across the whole length of the protein. However, there is a highly similar region of these proteins located in the first half of their central portion (54% identity, 85% similarity between positions 393 to 1620), while the N- and C-terminal portions of the proteins have relatively low sequence identity (https://github.com/GeiselBiofilm/Collins-MapA/tree/master/Supplemental_File_Alignments). This pattern is in contrast to the typically high conservation of the N and C termini and the low conservation of the central portion of LapA-like proteins (66, 67).

DISCUSSION

In this paper, we present MapA, a second type 1-secreted, large RTX adhesin that contributes to biofilm formation by *P. fluorescens*. We demonstrate that MapA is surface localized and can contribute to biofilm formation in the absence of LapA, at least under one growth condition we have identified to date. We also present genetic data showing that MapA surface localization is likely controlled by the previously described c-di-GMP effector protein, LapD, and the periplasmic protease, LapG (see model in Fig. 11A).

Our bioinformatic analysis indicates the distribution of similar multiple-adhesin

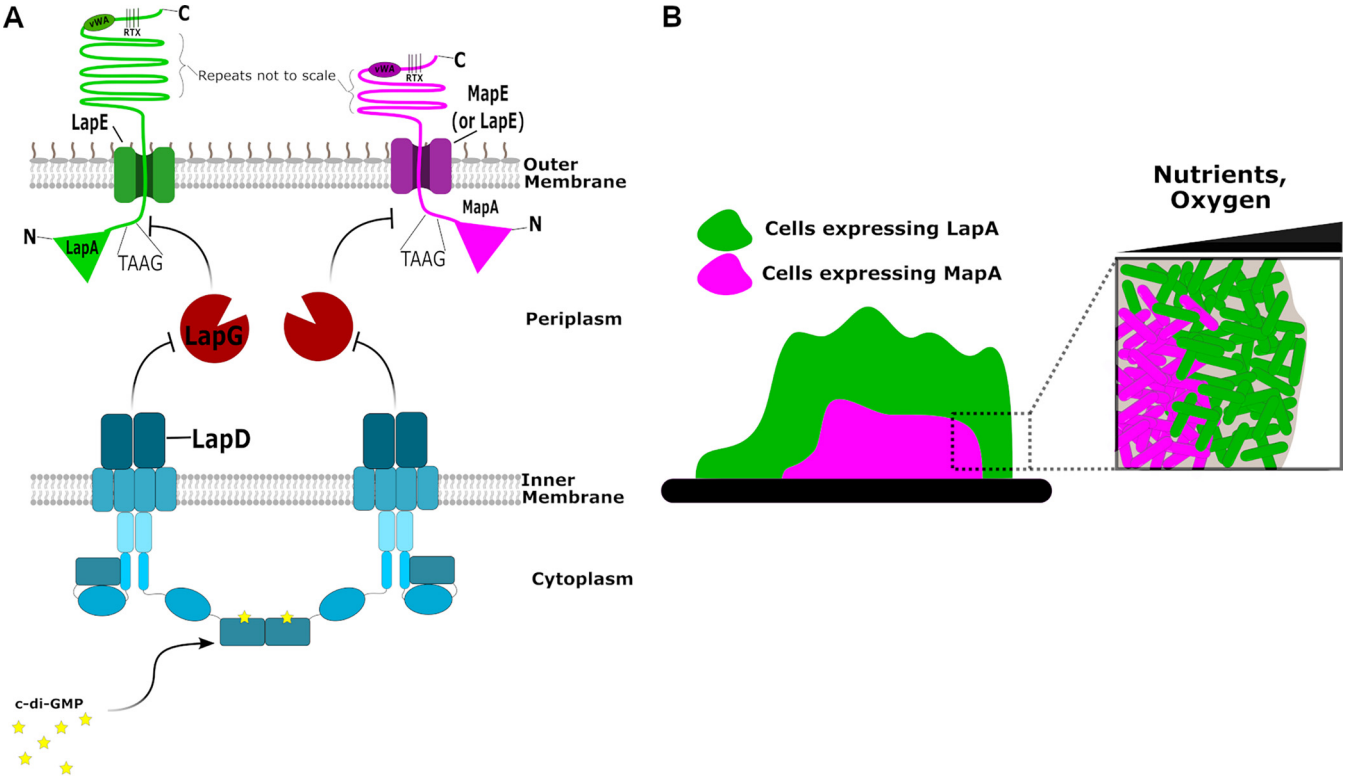

FIG 11 Model of the mechanisms by which LapA and MapA contribute to biofilm formation. (A) Model for c-di-GMP regulation of cell surface localization of LapA and MapA. Representations of the LapA (left) and MapA (right) adhesins anchored in the outer membrane via LapE and MapE, respectively, are shown. Also shown is the periplasmic protease LapG and the inner membrane, c-di-GMP receptor LapD, which regulates LapG activity. (B) Representation of the expression of *lapA* and *mapA* in a biofilm. Indicated are possible roles for nutrient and/or oxygen limitation in controlling the expression of the *mapA* gene.

systems throughout the *Proteobacteria*. Through our analysis, we identified many LapD and LapG homolog-encoding organisms whose genomes code for differing numbers of putative LapA-like proteins. However, we also identified many organisms that seem to encode LapD and LapG homologs but no identifiable LapA. Even within the *Pseudomonas* genus, we identified multiple species that seemed to lack any identifiable LapA- or MapA-like proteins (Fig. 10). It is possible that LapA-like proteins are present in these organisms and that our approach was not able to identify them or that the protein sequence database that we used as the source of our data is incomplete due to misannotation of these large, often repeat-rich proteins. In addition, the search parameters we used to identify LapA-like proteins are based on the characterization of a small number of proteins characterized to date (67), so it is possible that we have designed our search in such a way that some authentic LapA-like proteins were excluded. However, in the case of *P. aeruginosa*, a LapD and a LapG homolog are present but no LapA-like protein exists. Instead, LapG is able to proteolytically process a noncanonical target CdrA and regulate its localization to the cell surface (68). CdrA is secreted through a type Vb secretion process and is seemingly evolutionarily unrelated to LapA. Therefore, we hypothesize that some of the organisms we have identified that lack LapA-like proteins may encode proteins that have convergently evolved to be regulated by LapG. Thus, our analysis may provide a good basis on which to identify organisms that may encode other novel LapG-regulated proteins.

Interestingly, while both the *P. aeruginosa* and *P. fluorescens* lineages contain many organisms encoding LapD, LapG, and LapA-like proteins, the *P. pertucinogena* lineage contains only two such species. The presence of LapD and LapG homologs in organisms outside the *Pseudomonas* genus suggest that these proteins were lost in the *P. pertucinogena* lineage rather than gained in the other *Pseudomonas* lineages. *P. pertucinogena* lineage members are thought to be more niche specialized than other

Pseudomonas species and have reduced genome size and metabolic versatility (69–72). Thus, it is possible that the genome reduction that is thought to have occurred in the *P. pertucinogena* lineage is responsible for the apparent absence of LapD, LapG, and LapA-like proteins in these organisms.

Through our analysis of the sequence similarity between LapA-like proteins, we have found that many organisms both within the *Pseudomonas* genus and in other genera encode LapA-like proteins with high sequence similarity to LapA or MapA. Within the *Pseudomonas* genus, these LapA-like proteins often have high sequence similarity to LapA and MapA across the whole length of the protein, particularly within the *P. fluorescens* lineage. Organisms from other genera were found to encode LapA-like proteins with lower sequence similarity with LapA and MapA over the whole length of the protein. However, in some cases, portions of the central region of these proteins appear to be highly identical. The precise function of the diverse repeated sequences found in LapA-like proteins is poorly understood (67). In some cases, an extender-like function has been described which positions functional or substrate-binding domains of the protein away from the cell surface (61, 62). However, in the case of LapA, the repeats are thought to directly bind to hydrophobic surfaces (26). It is therefore possible that LapA-like proteins with high identity over parts of their central portion contain conserved substrate-binding domains or bind to surfaces with similar physical characteristics.

How MapA contributes to biofilm formation is still not entirely clear, and complicating our analysis is the fact that our genetic studies indicate that MapA may utilize the Lap secretion system for surface localization. Loss of MapA function results in a defect in biofilm formation in static 96-well dish assays, at least under a select medium condition. Similarly, MapA was required for robust biofilm formation in a microfluidic device. The phenotype of the *mapA* mutants is also clearly distinct from that of strains lacking LapA. What is the basis for this difference in phenotype? One obvious explanation is that the LapA protein is ~200 kDa larger than MapA, and there are clear differences in the sequence of the central repeat regions. Differential expression of the proteins might also impact their differential contributions to biofilm formation. For example, we observed differential spatial expression patterns of the *mapA* and *lapA* genes in biofilms grown in microfluidic chambers under flow. However, our studies using the Pswap construct, which allows *mapA* to be expressed via the *lapA* promoter, argue against this hypothesis. We note that *mapA* expression is seen only in large, thicker regions of biofilms, which presumably would be oxygen or nutrient limited. Thus, we postulate that oxygen, nutrients, or energy status of the cells may contribute to the regulation of *mapA* gene expression (Fig. 11B). This observation is consistent with the fact that loss of MapA shows a phenotype in static assays when only arginine is present but not when the medium contains a complex mixture of peptides and glycerol. Furthermore, given that arginine has been shown previously to stimulate the c-di-GMP level in pseudomonads (39, 41), the involvement of MapA in biofilm formation may also be a c-di-GMP-regulated process. Studies are ongoing to dissect the role of transcriptional regulation in the different roles of LapA and MapA in *P. fluorescens* biofilm formation.

Our findings here are reminiscent of previous studies with *P. putida*, which showed that this organism utilizes two adhesins during biofilm formation. The *P. putida* adhesins, LapA and LapF, are required for biofilm formation and play distinct roles in building the three-dimensional structure of the biofilm (6, 55–57). *P. putida* LapA is involved in initial attachment to the substratum, while LapF is required for the three-dimensional structure of the biofilm via contributing cellular cohesion (6, 45, 56, 57). It is possible that the LapA and MapA of *P. fluorescens* play similar roles. The *lapA* mutant of *P. fluorescens* has a reported defect in early biofilm formation (23, 25), and the data we present here show that MapA is likely produced only in the heart of a mature biofilm. Furthermore, the *mapA* mutant strain appears to initiate a biofilm, but that biofilm does not fully mature, a phenotype similar to that observed for the *lapF* mutant of *P. putida* (56). Interestingly, a key difference between the two strains is that

while the *P. putida* LapA protein is thought to be processed by LapG, LapF was not identified by our search for LapA-like proteins as it does not contain key features required for LapG processing. Thus, LapF may be part of a distinct class of LapA-like adhesins that are secreted and permanently anchored to the cell surface, as LapF appears to not be processed by LapG. Interestingly, we showed previously that the LapA-like PA1874 protein of *P. aeruginosa*, which shares features of the N-terminal retention module with the LapA protein of *P. fluorescens*, is also not processed by LapG and lacks the canonical TAAG processing site for LapG (29). Thus, Lap-like proteins which are cell surface localized but lacking LapG processing sites might be another variation on the theme of Lap-like adhesion systems. Finally, in *P. putida* KT2440, the *lapA* and *lapF* genes are differentially regulated by FleQ, RpoS, GacS/GacA, and Fis (56, 73–76). Our observation that MapA appears to be produced at high levels only in the center of the biofilm, which is typically associated with a region of the biofilm lacking nutrients, and in medium that promotes high levels of c-di-GMP production suggests that the *mapA* gene may also be under the control of RpoS and FleQ, respectively. Future studies should explore the role of these transcription factors in controlling expression of the *lapA* and *mapA* genes in *P. fluorescens*.

Our analysis here suggests that Lap-like systems are conserved across the pseudomonads and in other *Proteobacteria*. The observation that some pseudomonads and other *Proteobacteria* can express two discrete LapA-like proteins adds to the complex strategies that these bacteria can utilize to establish their extracellular matrix during biofilm formation. In the case of *P. fluorescens* and *P. putida*, their two respective LapA-like proteins appear to play distinct roles in biofilm initiation versus biofilm formation, likely driven in part by their distinct protein sequences and their differential regulation. While exopolysaccharides and extracellular DNA have received the majority of attention as matrix components, the observation that organisms like *P. fluorescens*, *P. putida*, *V. cholerae,* and *S. enterica* all use multiple adhesins to form a biofilm indicates the importance of such extracellular proteins as matrix components.

MATERIALS AND METHODS

Strains and media. The strains used in this study can be found in Table 3. *P. fluorescens* Pf0-1 and *E. coli* S17 (77, 78) were used throughout this study. *P. fluorescens* and *E. coli* were grown at 30°C when containing plasmids; *E. coli* strains were otherwise grown at 37°C. Media used in this study include lysogeny broth (LB), K10T-1 (77), and two new modifications of previously used media. The first, KA medium, is a modification of K10-T in which the changes are the removal of glycerol and tryptone and the addition of 0.4% (wt/vol) L-arginine HCl. The second medium was used for growing *P. fluorescens* Pf0-1 in microfluidic devices and is a modification of BMM medium that was previously described (51). This BMM medium was modified by reducing the concentration of glycerol and $(NH_4)_2SO_4$ by 16-fold and adding L-arginine. The final concentrations of each in this medium were therefore 0.009375% (vol/vol) glycerol, 472.5 μM $(NH_4)_2SO_4$, and 0.025% (wt/vol) L-arginine mono-HCl (Sigma). When *E. coli* was grown harboring the allelic exchange plasmid pMQ30 or the expression plasmid pMQ72, the growth medium was supplemented with 10 μg/μl gentamicin. When *E. coli* was grown harboring the plasmid pMQ56 or the helper plasmid pUX-BF13, the growth medium was supplemented with 50 μg/μl carbenicillin. When *P. fluorescens* was grown harboring pMQ72, the growth medium was supplemented with 30 μg/μl gentamicin. Allelic exchange was performed as previously reported (79).

Static biofilm assay. *Pseudomonas fluorescens* strains were struck out on LB plates overnight. Single colonies were picked and grown overnight in liquid LB medium with shaking. A 1.5-μl volume of overnight culture was added to 100 μl of growth medium in a 96-well U-bottom polystyrene plate (Costar). Plates were covered and placed in a humidified chamber at 30°C for either 6 or 16 h, as indicated, at which time the liquid in the wells was discarded and the wells were stained with 125 μl of 0.1% (wt/vol) crystal violet (CV) at room temperature for 20 min and then rinsed two times with water. Wells were allowed to dry, and then the stain was dissolved using 150 μl of a solution of water, methanol, and acetic acid (45:45:10 ratio by volume) for 10 min at room temperature. A 100-μl volume of the solubilized CV solution was transferred to a flat-bottom 96-well plate, and the optical density at 550 nm (OD_{550}) was recorded.

Construction of HA-tagged MapA. The 3×HA tag was amplified by PCR from *P. fluorescens* Pf0-1 in which LapA had been HA tagged. This tag was inserted into the genomic copy of the Pfl01_1463 (*mapA*) gene between the codon encoding H2601 and G2602 by allelic exchange, as previously described (79).

Assessment of surface localization of adhesins by dot blot. WT *P. fluorescens* Pf0-1 and mutants were grown with agitation in LB medium at 30°C for ~16 h, and then 100 μl of this inoculum was added to 25 ml of KA medium. This subculture was incubated with agitation at 30°C for 24 h. After incubation, the 25-ml cultures were centrifuged at 5,000 rpm for 5 min in a microcentrifuge, and cell pellets were

TABLE 3 Strains and plasmids used in this study

Strain or plasmid	Genotype or description	Reference or source
Strains		
Saccharomyces cerevisiae InvSc1	*MAT***a***/MAT leu2/leu2 trp1-289/trp1-289 ura3-52/ura3-52 his3D1/his3D1*	Invitrogen
Escherichia coli S17-1 (λpir)	Tp^r Sm^r *recA thi pro hsdR-M*+RP4::2-Tc::Mu::Km Tn*7* λ*pir*	78
Pseudomonas fluorescens Pf0-1		
SMC 1358	WT Pf0-1 (both LapA and MapA untagged)	
SMC 4798	LapA-HA; HA tag inserted after residue 4093	88
SMC 8581	MapA-HA	This study
SMC 7905	LapA-HA MapA-HA	This study
SMC 8586	Δ*lapA* MapA-HA	This study
SMC 7977	Δ*mapA* LapA-HA	This study
SMC 8570	Δ*lapA* Δ*mapA*	This study
SMC 8582	Δ*lapD* LapA-HA MapA-HA	This study
SMC 8584	Δ*lapG* LapA-HA MapA-HA	This study
SMC 8594	Δ*lapAG* MapA-HA	This study
SMC 8569	Δ*lapAG* Δ*mapA*	This study
SMC 8588	Δ*mapE* LapA-HA MapA-HA	This study
SMC 8589	Δ*lapA* Δ*mapE* MapA-HA	This study
SMC 8591	Δ*lapE* Δ*mapE* LapA-HA	This study
SMC 7954	Δ*lapE* LapA-HA	29
SMC 8636	Δ*lapE* Δ*mapA* LapA-HA	This study
SMC 8638	P_{mapA}::P_{lapA} (also known as Pswap) LapA-HA MapA-HA	This study
SMC 8639	Δ*lapA* P_{mapA}::P_{lapA} MapA-HA	This study
SMC 8642	mTn*7* P_{lapA}-GFP P_{mapA}-mCherry LapA-HA MapA-HA (also known as Pfluor)	This study
Plasmids		
SMC 7221	mTn*7*/pMQ56	79
SMC 1852	pUX-BF13 *tnsA tnsC tnsD tnsE mob ori* R6K *bla* MCS	89
SMC 2765	pMQ30	79
SMC 7975	pMQ30 Δ*mapA*	This study
SMC 7907	pMQ30 MapA-HA	This study
SMC 8703	pMQ30 Δ*mapE*	This study
SMC 8637	pMQ30 P_{mapA}::P_{mapA}	This study
SMC 8635	pMQ56 mTn*7* p*lapA*-GFP, p*mapA*-mCherry	This study

resuspended in 1 ml of fresh medium. All cultures were washed once with fresh medium and normalized such that the OD_{600} of each culture was the same. Five microliters of washed, normalized culture was spotted onto a nitrocellulose membrane and allowed to dry. The membrane was then incubated in blocking buffer for 1 h at 25°C (Tris-buffered saline [TBS] with Tween 20 [TBST] with 3% bovine serum albumin [BSA]; Sigma) before being probed for LapA or MapA containing an HA epitope tag with an anti-HA epitope tag antibody (BioLegend) at a 1:2,000 dilution in TBST with 3% BSA and 0.02% sodium azide overnight at 4°C. Excess antibody was washed away with 3× TBST rinses before the membrane was incubated with anti-mouse secondary antibody (Bio-Rad) conjugated to horseradish peroxidase at a 1:15,000 dilution in TBST at 25°C for 1 h. The membrane was then washed three times in TBST and once in TBS (Bio-Rad) before being exposed to 2 ml of Western Lightning Plus-ECL enhanced chemiluminescence substrate (PerkinElmer). The membrane was then exposed to BioMax XAR film (Carestream), and the film was processed on a Kodak X-Omat 2000 film processor. The processed films were scanned in grayscale, and the dots were quantified in ImageJ (NIH) by reversing the pixel values, defining a region of interest (ROI), and then using that defined object to measure the mean gray value of each spot and the background of the film, which was defined as an area of the film where no spot was present. The background measurement was subtracted from the mean pixel density of each spot.

Microfluidic devices. Microfluidic devices were constructed as previously described (80). Specifically, the devices were constructed by bonding polydimethylsiloxane (PDMS) castings to size #1.5, 36- by 60-mm cover glass (ThermoFisher, Waltham MA) (81, 82). Bacterial strains were grown in 5 ml of LB medium with 15 μg/μl gentamicin overnight at 30°C with agitation. A 300-μl volume of overnight culture was pelleted, and the supernatant was removed before being resuspended in 1 ml of the modified BMM medium described above. Strains were inoculated into channels of the microfluidic devices and allowed to colonize for 1 h at room temperature, 21 to 24°C, before a constant flow of 0.5 μl/min of the modified BMM (described above) was provided. Medium flow was achieved using syringe pumps (Pico Plus Elite; Harvard Apparatus) and 5-ml syringes (27-gauge needle) fitted with number 30 Cole-Palmer polytetrafluoroethylene (PTFE) tubing (inside diameter, 0.3 mm). Tubing was inserted into holes bored in the PDMS with a catheter punch driver.

Imaging. Biofilms were imaged using an Andor W1 spinning-disk confocal microscope, an Andor Zyla camera, and a Nikon Ti microscope. A 488-nm laser was used to excite GFP, while a 560-nm laser line was used to excite mRuby. Images were captured using Nikon NIS software.

LapD and LapG homolog prediction and LapA-like protein identification. The approach to identifying LapD- and LapG-encoding organisms and LapA-like proteins was modified from a previously

described approach (29). The code is posted at https://github.com/GeiselBiofilm/Collins-MapA. Briefly, LapG and LapD homologs were defined as ORF coding proteins with the pfam06035 and pfam16448 domains, respectively. The NCBI Conserved Domains Database (CDD) was utilized to generate a list of LapG- and LapD-encoding bacteria, and the programming language R (83) was used to determine the intersecting LapD- and LapG-encoding bacteria by text matching their species name identifiers. The protein annotations of these genomes were downloaded from the NCBI genome database, and each annotated locus with a size greater than 1,000 amino acids was interrogated for the presence of a LapG cleavage site within amino acids 70 to 150 [(T/A/P)AA(G/V)] and at least one RTX motif [DX(L/I)X4GXD X(L/I)XGGX3D].

Phylogenetic tree construction. Representatives of each *Pseudomonas* species in the GenBank database were selected based on genome quality (i.e., fully assembled genome, or highest N_{50} if genome in contigs or scaffolds). In the case of species for which multiple strains with high-quality genomes were available, common lab strain representatives were chosen. A list of the strains used in the construction of this tree is given in File S3 in the supplemental material. The genome assembly files were retrieved from the GenBank ftp server and used to construct a phylogenetic tree according to a previously described method, as follows (63, 64). Orthologs of the 16S rRNA, *gyrB*, *rpoB*, and *rpoD* genes were identified by BLASTn version 2.6.0 (using the setting −gapopen 2) using the sequences of *P. fluorescens* Pf0-1 genes as queries (Pfl01_R12, 16S rRNA; Pfl01_0004, *gyrB*; Pfl01_5086, *rpoB*; Pfl01_5149, *rpoD*). Any species for which no BLAST matches could be found for any of the query genes were removed. Multiple sequence alignment was conducted using MUSCLE version 3.8.31 (65) for each gene, and alignments were concatenated. Concatenated aligned sequences were analyzed using PAUP*4.0a (build 167) (84). Distance was calculated using a Jukes-Cantor model, and a tree was constructed using neighbor-joining.

Statistics. Statistical analysis was conducted in GraphPad Prism 8, and the statistical test performed is indicated in each figure legend or in the test. Unless otherwise indicated, each experiment was performed in at least triplicate, with three or more technical replicates per experiment.

SUPPLEMENTAL MATERIAL

Supplemental material is available online only.

SUPPLEMENTAL FILE 1, XLSX file, 1.2 MB.

SUPPLEMENTAL FILE 2, XLSX file, 0.1 MB.

SUPPLEMENTAL FILE 3, XLSX file, 0.03 MB.

ACKNOWLEDGMENTS

We thank Carey Nadell and his laboratory for assistance with microfluidic chambers and imaging.

The work was supported by NIH grant no. R01 GM123609 to G.A.O. We also acknowledge the Molecular Biology Core, which receives funding from a Norris Cotton Cancer Center Core grant from the NIH (no. P30-CA023108).

REFERENCES

1. Flemming H, Wuertz S. 2019. Bacteria and archaea on Earth and their abundance in biofilms. Nat Rev Microbiol 17:247–260. https://doi.org/10.1038/s41579-019-0158-9.
2. van Wolferen M, Orell A, Albers S. 2018. Archaeal biofilm formation. Nat Rev Microbiol 16:699–713. https://doi.org/10.1038/s41579-018-0058-4.
3. Fanning S, Mitchel A. 2012. Fungal biofilms. PLoS Pathog 8:e1002585. https://doi.org/10.1371/journal.ppat.1002585.
4. Mann EE, Wozniak DJ. 2012. *Pseudomonas* biofilm matrix composition and niche biology. FEMS Microbiol Rev 36:893–916. https://doi.org/10.1111/j.1574-6976.2011.00322.x.
5. Van Houdt R, Michiels CW. 2005. Role of bacterial cell surface structures in *Escherichia coli* biofilm formation. Res Microbiol 156:626–633. https://doi.org/10.1016/j.resmic.2005.02.005.
6. Martínez-Gil M, Quesada JM, Ramos-González MI, Soriano MI, de Cristóbal RE, Espinosa-Urgel M. 2013. Interplay between extracellular matrix components of *Pseudomonas putida* biofilms. Res Microbiol 164:382–389. https://doi.org/10.1016/j.resmic.2013.03.021.
7. Berk V, Fong JCN, Dempsey GT, Develioglu ON, Zhuang X, Liphardt J, Yildiz FH, Chu S. 2012. Molecular architecture and assembly principles of *Vibrio cholerae* biofilms. Science 337:236–239. https://doi.org/10.1126/science.1222981.
8. Götz F. 2002. *Staphylococcus* and biofilms. Mol Microbiol 43:1367–1378. https://doi.org/10.1046/j.1365-2958.2002.02827.x.
9. Whitchurch CB, Tolker-Nielsen T, Ragas PC, Mattick JS. 2002. Extracellular DNA required for bacterial biofilm formation. Science 295:1487–1487. https://doi.org/10.1126/science.295.5559.1487.
10. Cue D, Lei MG, Lee CY. 2012. Genetic regulation of the intercellular adhesion locus in staphylococci. Front Cell Infect Microbiol 2:38. https://doi.org/10.3389/fcimb.2012.00038.
11. Foster TJ, Geoghegan JA, Ganesh VK, Höök M. 2014. Adhesion, invasion and evasion: the many functions of the surface proteins of *Staphylococcus aureus*. Nat Rev Microbiol 12:49–62. https://doi.org/10.1038/nrmicro3161.
12. Hobley L, Harkins C, MacPhee CE, Stanley-Wall NR. 2015. Giving structure to the biofilm matrix: an overview of individual strategies and emerging common themes. FEMS Microbiol Rev 39:649–669. https://doi.org/10.1093/femsre/fuv015.
13. Fong JCN, Syed KA, Klose KE, Yildiz FH. 2010. Role of *Vibrio* polysaccharide (vps) genes in VPS production, biofilm formation and *Vibrio cholerae* pathogenesis. Microbiology 156:2757–2769. https://doi.org/10.1099/mic.0.040196-0.
14. Yildiz FH, Schoolnik GK. 1999. *Vibrio cholerae* O1 El Tor: identification of a gene cluster required for the rugose colony type, exopolysaccharide production, chlorine resistance, and biofilm formation. Proc Natl Acad Sci U S A 96:4028–4033. https://doi.org/10.1073/pnas.96.7.4028.
15. Fong JNC, Yildiz FH. 2015. Biofilm matrix proteins. Microbiol Spectr 3:3. https://doi.org/10.1128/microbiolspec.MB-0004-2014.
16. Olsén A, Jonsson A, Normark S. 1989. Fibronectin binding mediated by a novel class of surface organelles on *Escherichia coli*. Nature 338:652–655. https://doi.org/10.1038/338652a0.
17. Vogeleer P, Tremblay YDN, Mafu AA, Jacques M, Harel J. 2014. Life on the outside: role of biofilms in environmental persistence of Shiga-toxin producing *Escherichia coli*. Front Microbiol 5:317. https://doi.org/10.3389/fmicb.2014.00317.
18. Ramey BE, Koutsoudis M, von Bodman SB, Fuqua C. 2004. Biofilm

formation in plant-microbe associations. Curr Opin Microbiol 7:602–609. https://doi.org/10.1016/j.mib.2004.10.014.
19. Zampini M, Pruzzo C, Bondre VP, Tarsi R, Cosmo M, Bacciaglia A, Chhabra A, Srivastava R, Srivastava BS. 2005. *Vibrio cholerae* persistence in aquatic environments and colonization of intestinal cells: involvement of a common adhesion mechanism. FEMS Microbiol Lett 244:267–273. https://doi.org/10.1016/j.femsle.2005.01.052.
20. Donlan RM. 2001. Biofilm formation: a clinically relevant microbiological process. Clin Infect Dis 33:1387–1392. https://doi.org/10.1086/322972.
21. Tamayo R, Patimalla B, Camilli A. 2010. Growth in a biofilm induces a hyperinfectious phenotype in *Vibrio cholerae*. Infect Immun 78:3560–3569. https://doi.org/10.1128/IAI.00048-10.
22. Høiby N. 2014. A personal history of research on microbial biofilms and biofilm infections. Pathog Dis 70:205–211. https://doi.org/10.1111/2049-632X.12165.
23. Hinsa SM, Espinosa-Urgel M, Ramos JL, O'Toole GA. 2003. Transition from reversible to irreversible attachment during biofilm formation by *Pseudomonas fluorescens* WCS365 requires an ABC transporter and a large secreted protein. Mol Microbiol 49:905–918. https://doi.org/10.1046/j.1365-2958.2003.03615.x.
24. Ivanov IE, Boyd CD, Newell PD, Schwartz ME, Turnbull L, Johnson MS, Whitchurch CB, O'Toole GA, Camesano TA. 2012. Atomic force and super-resolution microscopy support a role for LapA as a cell-surface biofilm adhesin of *Pseudomonas fluorescens*. Res Microbiol 163:685–691. https://doi.org/10.1016/j.resmic.2012.10.001.
25. Boyd CD, Smith TJ, El-Kirat-Chatel S, Newell PD, Dufrêne YF, O'Toole GA. 2014. Structural features of the *Pseudomonas fluorescens* biofilm adhesin LapA required for LapG-dependent cleavage, biofilm formation, and cell surface localization. J Bacteriol 196:2775–2788. https://doi.org/10.1128/JB.01629-14.
26. El-Kirat-Chatel S, Beaussart A, Boyd CD, O'Toole GA, Dufrêne YF. 2014. Single-cell and single-molecule analysis deciphers the localization, adhesion, and mechanics of the biofilm adhesin LapA. ACS Chem Biol 9:485–494. https://doi.org/10.1021/cb400794e.
27. El-Kirat-Chatel S, Boyd CD, O'Toole GA, Dufrêne YF. 2014. Single-molecule analysis of *Pseudomonas fluorescens* footprints. ACS Nano 8:1690–1698. https://doi.org/10.1021/nn4060489.
28. Newell PD, Boyd CD, Sondermann H, O'Toole GA. 2011. A c-di-GMP effector system controls cell adhesion by inside-out signaling and surface protein cleavage. PLoS Biol 9:e1000587. https://doi.org/10.1371/journal.pbio.1000587.
29. Smith TJ, Font ME, Kelly CM, Sondermann H, O'Toole GA. 2018. An N-terminal retention module anchors the giant adhesin LapA of *Pseudomonas fluorescens* at the cell surface: a novel subfamily of type I secretion systems. J Bacteriol 200:e00734-17. https://doi.org/10.1128/JB.00734-17.
30. Hinsa SM, O'Toole GA. 2006. Biofilm formation by *Pseudomonas fluorescens* WCS365: a role for LapD. Microbiology 152:1375–1383. https://doi.org/10.1099/mic.0.28696-0.
31. Newell PD, Monds RD, O'Toole GA. 2009. LapD is a bis-(3′,5′)-cyclic dimeric GMP-binding protein that regulates surface attachment by *Pseudomonas fluorescens* Pf0-1. Proc Natl Acad Sci U S A 106:3461–3466. https://doi.org/10.1073/pnas.0808933106.
32. Boyd CD, Chatterjee D, Sondermann H, O'Toole GA. 2012. LapG, required for modulating biofilm formation by *Pseudomonas fluorescens* Pf0-1, is a calcium-dependent protease. J Bacteriol 194:4406–4414. https://doi.org/10.1128/JB.00642-12.
33. Chatterjee D, Boyd CD, O'Toole GA, Sondermann H. 2012. Structural characterization of a conserved, calcium-dependent periplasmic protease from *Legionella pneumophila*. J Bacteriol 194:4415–4425. https://doi.org/10.1128/JB.00640-12.
34. Cooley RB, O'Donnell JP, Sondermann H. 2016. Coincidence detection and bi-directional transmembrane signaling control a bacterial second messenger receptor. Elife 5:e21848. https://doi.org/10.7554/eLife.21848.
35. Navarro MVAS, Newell PD, Krasteva PV, Chatterjee D, Madden DR, O'Toole GA, Sondermann H. 2011. Structural basis for c-di-GMP-mediated inside-out signaling controlling periplasmic proteolysis. PLoS Biol 9:e1000588. https://doi.org/10.1371/journal.pbio.1000588.
36. Ude S, Arnold DL, Moon CD, Timms-Wilson T, Spiers AJ. 2006. Biofilm formation and cellulose expression among diverse environmental *Pseudomonas* isolates. Environ Microbiol 8:1997–2011. https://doi.org/10.1111/j.1462-2920.2006.01080.x.
37. Spiers AJ, Bohannon J, Gehrig SM, Rainey PB. 2003. Biofilm formation at the air-liquid interface by the *Pseudomonas fluorescens* SBW25 wrinkly spreader requires an acetylated form of cellulose. Mol Microbiol 50:15–27. https://doi.org/10.1046/j.1365-2958.2003.03670.x.
38. Liu Z, Beskrovnaya P, Melnyk RA, Hossain SS, Khorasani S, O'Sullivan LR, Wiesmann CL, Bush J, Richard JD, Haney CH. 2018. A genome-wide screen identifies genes in rhizosphere-associated *Pseudomonas* required to evade plant defenses. mBio 9:e00433-18. https://doi.org/10.1128/mBio.00433-18.
39. Caiazza NC, O'Toole GA. 2004. SadB is required for the transition from reversible to irreversible attachment during biofilm formation by *Pseudomonas aeruginosa* PA14. J Bacteriol 186:4476–4485. https://doi.org/10.1128/JB.186.14.4476-4485.2004.
40. Ramos-González MI, Travieso ML, Soriano MI, Matilla MA, Huertas-Rosales Ó, Barrientos-Moreno L, Tagua VG, Espinosa-Urgel M. 2016. Genetic dissection of the regulatory network associated with high c-di-GMP levels in *Pseudomonas putida* KT2440. Front Microbiol 7:1093. https://doi.org/10.3389/fmicb.2016.01093.
41. Bernier SP, Ha D-G, Khan W, Merritt JH, O'Toole GA. 2011. Modulation of *Pseudomonas aeruginosa* surface-associated group behaviors by individual amino acids through c-di-GMP signaling. Res Microbiol 162:680–688. https://doi.org/10.1016/j.resmic.2011.04.014.
42. Sulochana M. 1962. Amino acids in root exudates of cotton. Plant Soil 16:312–326. https://doi.org/10.1007/BF01381342.
43. Gitte RR, Rai PV, Patil RB. 1978. Chemotaxis of *Rhizobium* sp. towards root exudate of *Cicer arietinum* L. Plant Soil 50:553–566. https://doi.org/10.1007/BF02107208.
44. Collins JC, Reilly EJ. 1968. Chemical composition of the exudate from excised maize roots. Planta 83:218–222. https://doi.org/10.1007/BF00385025.
45. Fuqua C. 2010. Passing the baton between laps: adhesion and cohesion in *Pseudomonas putida* biofilms. Mol Microbiol 77:533–536. https://doi.org/10.1111/j.1365-2958.2010.07250.x.
46. Touzé T, Eswaran J, Bokma E, Koronakis E, Hughes C, Koronakis V. 2004. Interactions underlying assembly of the *Escherichia coli* AcrAB-TolC multidrug efflux system. Mol Microbiol 53:697–706. https://doi.org/10.1111/j.1365-2958.2004.04158.x.
47. Létoffé S, Delepelaire P, Wandersman C. 1996. Protein secretion in gram-negative bacteria: assembly of the three components of ABC protein-mediated exporters is ordered and promoted by substrate binding. EMBO J 15:5804–5811. https://doi.org/10.1002/j.1460-2075.1996.tb00967.x.
48. Kobayashi N, Nishino K, Yamaguchi A. 2001. Novel macrolide-specific ABC-type efflux transporter in *Escherichia coli*. J Bacteriol 183:5639–5644. https://doi.org/10.1128/JB.183.19.5639-5644.2001.
49. Tikhonova EB, Dastidar V, Rybenkov VV, Zgurskaya HI. 2009. Kinetic control of TolC recruitment by multidrug efflux complexes. Proc Natl Acad Sci U S A 106:16416–16421. https://doi.org/10.1073/pnas.0906601106.
50. Wandersman C, Delepelaire P. 1990. TolC, an *Escherichia coli* outer membrane protein required for hemolysin secretion. Proc Natl Acad Sci U S A 87:4776–4780. https://doi.org/10.1073/pnas.87.12.4776.
51. Dahlstrom KM, Collins AJ, Doing G, Taroni JN, Gauvin TJ, Greene CS, Hogan DA, O'Toole GA. 2018. A multimodal strategy used by a large c-di-GMP network. J Bacteriol 200:e00703-17. https://doi.org/10.1128/JB.00703-17.
52. van der Velden AW, Bäumler AJ, Tsolis RM, Heffron F. 1998. Multiple fimbrial adhesins are required for full virulence of *Salmonella typhimurium* in mice. Infect Immun 66:2803–2808. https://doi.org/10.1128/IAI.66.6.2803-2808.1998.
53. Latasa C, Roux A, Toledo-Arana A, Ghigo J-M, Gamazo C, Penadés JR, Lasa I. 2005. BapA, a large secreted protein required for biofilm formation and host colonization of *Salmonella enterica* serovar Enteritidis. Mol Microbiol 58:1322–1339. https://doi.org/10.1111/j.1365-2958.2005.04907.x.
54. Morgan E, Bowen AJ, Carnell SC, Wallis TS, Stevens MP. 2007. SiiE is secreted by the *Salmonella enterica* serovar Typhimurium pathogenicity island 4-encoded secretion system and contributes to intestinal colonization in cattle. Infect Immun 75:1524–1533. https://doi.org/10.1128/IAI.01438-06.
55. Espinosa-Urgel M, Salido A, Ramos J-L. 2000. Genetic analysis of functions involved in adhesion of *Pseudomonas putida* to seeds. J Bacteriol 182:2363–2369. https://doi.org/10.1128/jb.182.9.2363-2369.2000.
56. Martínez-Gil M, Yousef-Coronado F, Espinosa-Urgel M. 2010. LapF, the second largest *Pseudomonas putida* protein, contributes to plant root colonization and determines biofilm architecture. Mol Microbiol 77:549–561. https://doi.org/10.1111/j.1365-2958.2010.07249.x.

57. Martínez-Gil M, Romero D, Kolter R, Espinosa-Urgel M. 2012. Calcium causes multimerization of the large adhesin LapF and modulates biofilm formation by *Pseudomonas putida*. J Bacteriol 194:6782–6789. https://doi.org/10.1128/JB.01094-12.
58. Kitts G, Giglio KM, Zamorano-Sánchez D, Park JH, Townsley L, Cooley RB, Wucher BR, Klose KE, Nadell CD, Yildiz FH, Sondermann H. 2019. A conserved regulatory circuit controls large adhesins in *Vibrio cholerae*. mBio 10:e02822-19. https://doi.org/10.1128/mBio.02822-19.
59. Ambrosis N, Boyd CD, ÓToole GA, Fernández J, Sisti F. 2016. Homologs of the LapD-LapG c-di-GMP effector system control biofilm formation by *Bordetella bronchiseptica*. PLoS One 11:e0158752. https://doi.org/10.1371/journal.pone.0158752.
60. Pérez-Mendoza D, Coulthurst SJ, Humphris S, Campbell E, Welch M, Toth IK, Salmond G. 2011. A multi-repeat adhesin of the phytopathogen, *Pectobacterium atrosepticum*, is secreted by a type I pathway and is subject to complex regulation involving a non-canonical diguanylate cyclase. Mol Microbiol 82:719–733. https://doi.org/10.1111/j.1365-2958.2011.07849.x.
61. Guo S, Stevens CA, Vance TDR, Olijve LLC, Graham LA, Campbell RL, Yazdi SR, Escobedo C, Bar-Dolev M, Yashunsky V, Braslavsky I, Langelaan DN, Smith SP, Allingham JS, Voets IK, Davies PL. 2017. Structure of a 1.5-MDa adhesin that binds its Antarctic bacterium to diatoms and ice. Sci Adv 3:e1701440. https://doi.org/10.1126/sciadv.1701440.
62. Vance TDR, Graham LA, Davies PL. 2018. An ice-binding and tandem beta-sandwich domain-containing protein in *Shewanella frigidimarina* is a potential new type of ice adhesin. FEBS J 285:1511–1527. https://doi.org/10.1111/febs.14424.
63. Peix A, Ramírez-Bahena M-H, Velázquez E. 2018. The current status on the taxonomy of *Pseudomonas* revisited: an update. Infect Genet Evol 57:106–116. https://doi.org/10.1016/j.meegid.2017.10.026.
64. Mulet M, Lalucat J, García-Valdés E. 2010. DNA sequence-based analysis of the *Pseudomonas* species. Environ Microbiol 12:1513–1530. https://doi.org/10.1111/j.1462-2920.2010.02181.x.
65. Edgar RC. 2004. MUSCLE: multiple sequence alignment with high accuracy and high throughput. Nucleic Acids Res 32:1792–1797. https://doi.org/10.1093/nar/gkh340.
66. Smith TJ, Sondermann H, O'Toole GA. 2018. Type 1 does the two-step: type 1 secretion substrates with a functional periplasmic intermediate. J Bacteriol 200:e00168-18. https://doi.org/10.1128/JB.00168-18.
67. Collins AJ, Smith TJ, Sondermann H, O'Toole GA. From input to output: the Lap/c-di-GMP biofilm regulatory circuit. Annu Rev Microbiol, in press.
68. Cooley RB, Smith TJ, Leung W, Tierney V, Borlee BR, O'Toole GA, Sondermann H. 2016. Cyclic di-GMP-regulated periplasmic proteolysis of a *Pseudomonas aeruginosa* type Vb secretion system substrate. J Bacteriol 198:66–76. https://doi.org/10.1128/JB.00369-15.
69. Bollinger A, Thies S, Katzke N, Jaeger K-E. 2020. The biotechnological potential of marine bacteria in the novel lineage of *Pseudomonas pertucinogena*. Microb Biotechnol 13:19–31. https://doi.org/10.1111/1751-7915.13288.
70. Kawai Y, Yabuuchi E. 1975. *Pseudomonas pertucinogena* sp. nov., an organism previously misidentified as *Bordetella pertussis*. Int J Syst Evol Microbiol 25:317–323. https://doi.org/10.1099/00207713-25-4-317.
71. Sánchez D, Mulet M, Rodríguez AC, David Z, Lalucat J, García-Valdés E. 2014. *Pseudomonas aestusnigri* sp. nov., isolated from crude oil-contaminated intertidal sand samples after the Prestige oil spill. Syst Appl Microbiol 37:89–94. https://doi.org/10.1016/j.syapm.2013.09.004.
72. Mulet M, Sánchez D, Rodríguez AC, Nogales B, Bosch R, Busquets A, Gomila M, Lalucat J, García-Valdés E. 2018. *Pseudomonas gallaeciensis* sp. nov., isolated from crude-oil-contaminated intertidal sand samples after the Prestige oil spill. Syst Appl Microbiol 41:340–347. https://doi.org/10.1016/j.syapm.2018.03.008.
73. Moor H, Teppo A, Lahesaare A, Kivisaar M, Teras R. 2014. Fis overexpression enhances *Pseudomonas putida* biofilm formation by regulating the ratio of LapA and LapF. Microbiology 160:2681–2693. https://doi.org/10.1099/mic.0.082503-0.
74. Ainelo H, Lahesaare A, Teppo A, Kivisaar M, Teras R. 2017. The promoter region of *lapA* and its transcriptional regulation by Fis in *Pseudomonas putida*. PLoS One 12:e0185482. https://doi.org/10.1371/journal.pone.0185482.
75. Blanco-Romero E, Redondo-Nieto M, Martínez-Granero F, Garrido-Sanz D, Ramos-González MI, Martín M, Rivilla R. 2018. Genome-wide analysis of the FleQ direct regulon in *Pseudomonas fluorescens* F113 and *Pseudomonas putida* KT2440. Sci Rep 8:13145. https://doi.org/10.1038/s41598-018-31371-z.
76. Martínez-Gil M, Ramos-González MI, Espinosa-Urgel M. 2014. Roles of cyclic di-GMP and the Gac system in transcriptional control of the genes coding for the *Pseudomonas putida* adhesins LapA and LapF. J Bacteriol 196:1484–1495. https://doi.org/10.1128/JB.01287-13.
77. Monds RD, Newell PD, Schwartzman JA, O'Toole GA. 2006. Conservation of the Pho regulon in *Pseudomonas fluorescens* Pf0-1. Appl Environ Microbiol 72:1910–1924. https://doi.org/10.1128/AEM.72.3.1910-1924.2006.
78. Simon R, Priefer U, Pühler A. 1983. A broad host range mobilization system for in vivo genetic engineering: transposon mutagenesis in gram negative bacteria. Nat Biotechnol 1:784–791. https://doi.org/10.1038/nbt1183-784.
79. Shanks RMQ, Caiazza NC, Hinsa SM, Toutain CM, O'Toole GA. 2006. *Saccharomyces cerevisiae*-based molecular tool kit for manipulation of genes from gram-negative bacteria. Appl Environ Microbiol 72:5027–5036. https://doi.org/10.1128/AEM.00682-06.
80. Simmons M, Bond M, Drescher K, Bucci V, Nadell CD. 2019. Evolutionary dynamics of phage resistance in bacterial biofilms. bioRxiv https://doi.org/10.1101/552265.
81. Weibel DB, Diluzio WR, Whitesides GM. 2007. Microfabrication meets microbiology. Nat Rev Microbiol 5:209–218. https://doi.org/10.1038/nrmicro1616.
82. Sia SK, Whitesides GM. 2003. Microfluidic devices fabricated in poly(dimethylsiloxane) for biological studies. Electrophoresis 24:3563–3576. https://doi.org/10.1002/elps.200305584.
83. R Core Team. 2019. R: a language and environment for statistical computing. R Foundation for Statistical Computing, Vienna, Austria.
84. Swofford DL. 2003. PAUP*: phylogenetic analysis using parsimony (and other methods), version 4. Sinauer Associates, Sunderland, MA.
85. Waterhouse AM, Procter JB, Martin DMA, Clamp M, Barton GJ. 2009. Jalview Version 2—a multiple sequence alignment editor and analysis workbench. Bioinformatics 25:1189–1191. https://doi.org/10.1093/bioinformatics/btp033.
86. García-Valdés E, Lalucat J. 2016. Pseudomonas: molecular phylogeny and current taxonomy, p 1–23. *In* Pseudomonas: molecular and applied biology. Springer, New York, NY.
87. Horsman ME, Marous DR, Li R, Oliver RA, Byun B, Emrich SJ, Boggess B, Townsend CA, Mobashery S. 2017. Whole-genome shotgun sequencing of two β-proteobacterial species in search of the bulgecin biosynthetic cluster. ACS Chem Biol 12:2552–2557. https://doi.org/10.1021/acschembio.7b00687.
88. Monds RD, Newell PD, Gross RH, O'Toole GA. 2007. Phosphate-dependent modulation of c-di-GMP levels regulates *Pseudomonas fluorescens* Pf0-1 biofilm formation by controlling secretion of the adhesin LapA. Mol Microbiol 63:656–679. https://doi.org/10.1111/j.1365-2958.2006.05539.x.
89. Bao Y, Lies DP, Fu H, Roberts GP. 1991. An improved Tn7-based system for the single-copy insertion of cloned genes into chromosomes of gram-negative bacteria. Gene 109:167–168. https://doi.org/10.1016/0378-1119(91)90604-a.